University of Crete
Medical School
M. Sc. Program

Graduate program
mbhd
University of Crete Medical School

BRFAA
BIOMEDICAL RESEARCH FOUNDATION
ACADEMY OF ATHENS

Study on the role of adipose tissue regulatory T cells in tumor development and response to immunotherapy

Neofotistou-Themeli Elpida
M.Sc. Thesis

Supervisor: P. Verginis

Heraklion, July 2020

University of Crete
Medical School
M. Sc. Program

Graduate program
mbhd
University of Crete Medical School

BRFAA
BIOMEDICAL RESEARCH FOUNDATION
ACADEMY OF ATHENS

Μελέτη του ρόλου των ρυθμιστικών Τ κυττάτων του λιπώδους ιστού στην ανάπτυξη όγκου και την απόκριση σε ανοσοθεραπεία

Νεοφωτίστου-Θέμελη Ελπίδα
Διπλωματική Εργασία

Επιβλέπων: Π. Βεργίνης

Ηράκλειο, Ιούλιος 2020

Table of Contents

1.1 Abstract

Regulatory T cells (Tregs) are pivotal in maintaining peripheral tolerance and immune homeostasis. They are recruited to the tumor microenvironment during tumor progression, facilitating its escape from immune surveillance. They abundantly express immune checkpoint molecules, namely PD-1 and CTLA-4, and are thus the main targets for immunotherapy treatments. Tregs within the visceral adipose tissue (VAT) confer protective effects against metabolic dysfunction in obesity and are reprogrammed in obesity-related inflammation. Links between obesity and cancer have already been established as metabolic dysregulation has been correlated with increased cancer incidence, aggressive tumor progression and adverse prognosis in human patients. On the other hand, improved responses to cancer immunotherapy have been reported for overweight and mildly obese individuals. To date, the mechanisms underlying this paradox remain to be elucidated.

In this master thesis, we set out to explore the role of VAT Tregs in tumor progression and the development of anti-tumor immune responses, as well as in the responsiveness to immunotherapy. Our results suggest that diet-induced obesity accelerates B16.F10 melanoma progression in both male and female mice. Tumor-draining lymph nodes in obese mice display increased cellularity, though no differences are observed in the content of T cell subpopulations. The obese tumor T cell profile implies increased immune activity with reduced Treg over T effector ratios, though an overall decrease in the total number of infiltrating leukocytes correlated with the notable accelerated tumor progression. In the visceral adipose tissue there's evidence of immune suppression, indicated by a trend for increased PD-1 levels on Tregs and $CD8^+$ T cells alike, intensity of CTLA-4 signal on Tregs and Treg/T effector analogy, though total $CD45^+$ infiltration was slightly increased. We also report that, although the described effects were more prominent in males than females, the trends were for the most part comparable in both genders. Identification of specific molecular signatures in VAT Tregs during tumor development and also comparisons of the transcriptome of VAT and tumor-infiltrating Tregs will shed light in the contribution of obesity and specifically on obesity-related Tregs in cancer.

Overall, the inclusive approach of organismal immunometabolism acknowledges the innate implications of different systems and their combined effects on health and disease. In this light, unveiling the underlying mechanisms defining obesity and its effects on tumor responses and immunotherapy effectiveness, as well as the possible implications of VAT Tregs in this interplay would serve the dual purpose of providing immense clinical benefit but also propel our basic understanding of the intricate cross-talk between immune cell populations.

1.2 Abstract

Τα Τ ρυθμιστικά κύτταρα (Tregs) παίζουν σημαντικό ρόλο στη διατήρηση της περιφερικής ανοχής και της ομοιοστασίας των ανοσολογικών αντιδράσεων. Κατά την ανάπτυξη ενός όγκου, Tregs συσσωρεύονται στο μικροπεριβάλλον του και τον προστατεύουν από τους ανοσολογικούς μηχανισμούς του οργανισμού. Τα Tregs εκφράζουν σε μεγάλο ποσοστό ρυθμιστικά ανοσολογικά μόρια, κατά βάση PD-1 και CTLA-4, γεγονός που τα καθιστά βασικό στόχο της ανοσοθεραπείας. Στο σπλαχνικό λιπώδη ιστό, τα εγκατεστημένα Tregs έχουν διακριτό μοριακό αποτύπωμα και προστατευτικές δράσεις έναντι των μεταβολικών δυσλειτουργιών στην παχυσαρκία και τη χρόνια φλεγμονή που τη χαρακτηρίζει, ενώ επαναπρογραμματίζονται σε καταστάσεις μεταβολικής ανομοιοστασίας. Πληθώρα στοιχείων συνδέουν πλέον την παχυσαρκία με την εμφάνιση καρκίνου, και την καθιστούν έναν από τους βασικούς παράγοντες κινδύνου για επιθετικότερες εκφάνσεις της ασθένειας και δυσμενείς προγνώσεις σε ασθενείς. Ωστόσο, υπέρβαρα και ελαφρώς παχύσαρκα άτομα φαίνεται να ανταποκρίνονται περισσότερο στην ανοσοθεραπεία, παρότι οι μηχανισμοί πίσω από αυτό το παράδοξο δεν έχουν ακόμη διαλευκανθεί.

Στα πλαίσια αυτής της διπλωματικής εργασίας, στοχεύσαμε στην ανάλυση του ρόλου των ρυθμιστικών κυττάρων του σπλαχνικού λιπώδους ιστού (VAT Tregs) στην ανάπτυξη όγκου και τις ανοσολογικές αντιδράσεις εναντίον του, καθώς και στην ανοσοθεραπεία. Τα δεδομένα μας υποδεικνύουν ότι δίαιτα υψηλή σε λιπαρά ευνοεί την ανάπτυξη όγκου στο μοντέλο μελανώματος B16.F10 σε ποντίκια και των δύο φύλων. Οι λεμφαδένες-φρουροί στα παχύσαρκα ποντίκια παρουσιάζουν αύξηση του συνολικού αριθμού Τ κυττάρων, χωρίς ωστόσο να παρατηρείται κάποια διαφορά μεταξύ των συχνοτήτων των κυτταρικών υποπληθυσμών. Όσον αφορά στον ίδιο τον όγκο, το προφίλ των Τ κυττάρων στα παχύσαρκα ποντίκια μοιάζει να γίνεται πιο ανοσογονικό, με μικρότερους λόγους Tregs/T effectors, παρά τη συνολική μείωση των ανοσοκυττάρων που εισχωρούν στο μικροπεριβάλλον του**.** Στο λιπώδη ιστό, υπάρχουν δεδομένα μεγαλύτερης ανοσοανοχής, όπως φαίνεται από την αύξηση της έκφρασης του PD-1στα τα Tregs και τα $CD8^+$ κυτταροτοξικά Τ, την ένταση φθορισμού του CTLA-4 στα Tregs και την αναλογία Tregs/T effectors, παρότι το σύνολο των $CD45^+$ λεμφοκυττάρων αυξάνεται. Τα ευρήματά μας αποκαλύπτουν επίσης ότι οι τάσεις αυτές είναι συγκρίσιμες και για τα δύο φύλα, αν και πιο έντονες στα αρσενικά. Ο προσδιορισμός συγκεκριμένων μοριακών υπογραφών στα Tregs κατά την ανάπτυξη όγκου και συγκρίσεις του μεταγραφώματος των Tregs του λιπώδους ιστού και του μικροπεριβάλλοντος του όγκου θα μας έδιναν περισσότερες πληροφορίες για τη συνεισφορά της παχυσαρκίας, και συγκεκριμένα των Tregs του λιπώδους ιστού, στον καρκίνο.

Συνολικά, η προσέγγιση του ανοσομεταβολισμού αναγνωρίζει τη συνεισφορά διαφορετικών συστημάτων σε μία κατάσταση και τα συνδυαστικά τους αποτελέσματα σε φυσιολογικές και παθολογικές καταστάσεις. Λαμβάνοντας αυτό υπόψη, κρίνουμε σημαντικό να ανακαλύψουμε τους υποκείμενους μηχανισμούς που χαρακτηρίζουν την παχυσαρκία και τη συνεισφορά της στην πρόοδο του όγκου και την αποκρισιμότητα στην ανοσοθεραπεία, καθώς και τον πιθανό ρόλο των Tregs σε αυτή την αλληλεπίδραση. Ο στόχος αυτός έχει διπλή σημασία, καθώς αφενός θα προσέφερε κλινικά πλεονεκτήματα και αφετέρου θα εμπλούτιζε τη βασική μας κατανόηση των πολύπλοκων αλληλεπιδράσεων μεταξύ ανοσολογικών πληθυσμών.

2. Introduction

2.1 The Adipose Tissue

For a number of years the adipose tissue was considered as a type of loose connective tissue filled with lipid droplets contained within adipocytes, though no light was shed on its precise properties or its importance. It wasn't until several decades ago that its complexity was re-evaluated, as its morphology was better characterized and evidence emerged regarding its capacity to affect systemic nutrient homeostasis by storing calories after feeding and circulating free fatty acids during fasting. The discovery of adipose-derived serum factors such as adiponectin, leptin and TNFα revealed a role for adipose tissue as an endocrine organ indispensable for metabolic functions and energy homeostasis [1].

Though its core function is maintaining energy balance and lipid storage, adipose tissue has also been found to provide nutrients and hormonal signals that regulate the hypothalamic-pituitary-gonadal axis in both genders [2]. Additionally, it provides a layer of protection for sensitive organs such as the eyes, and structures exposed to mechanical stress, such as the calcaneus bone of the lower extremities in humans. Its morphology serves also in the insulation of the mammalian internal organs and thermoregulation.

It is now known that regarding the adipose tissue as homogeneous is a simplistic view, as in the mammalian body it is divided into distinct adipose depots with different tissue characteristics, cell population compositions and functions [3]. Many diseases affecting adipose tissue show depot-specific effects. Glucocorticoid excess due to endogenous overproduction or pharmacological treatments, for instance, involves redistribution of fat to visceral sites with simultaneous wasting of subcutaneous fat, as is the case with acquired lipodystrophy caused by anti-HIV medication. Congenital lipodystrophy also affects specific depots differentially, and different patterns of fat loss are observed, depending on specific genetic lesions.

Traditionally, adipocytes are divided into two categories; white adipocytes are unilocular, lipid-storing cells that make up depots of white adipose tissue (WAT), while brown adipocytes are smaller in size, multilocular, and involved in energy expenditure in specialized regions of brown adipose tissue (BAT).

Brown adipose tissue is highly specialized in non-shivering adaptive thermogenesis, and has been found only in placental mammals. Brown adipocytes are densely irrigated and rich in mitochondria, while expressing high levels of uncoupling protein-1 (UCP-1), a long chain fatty acid and proton co-transporter uncoupling fuel oxydation from ATP synthesis. Classical brown adipocytes are clustered in the interscapular, perirenal and spinal regions of rodents and humans.

Further studies in the different adipose tissues revealed an intermediate type of adipose tissue besides white and brown. Beige fat is adrenergically inducible, and beige adipocytes are dispersed throughout white adipose tissue depots. This type of adipose tissue displays greater variability in lipid droplet size and a greater proportion of lipid droplets as opposed to mitochondria compared to white fat and has a distinct trancriptional profile and adipocyte progenitors [4].

During the differentiation of white adipose tissue, which comprises the majority of total fat for most animals, distinct transcriptional profiles of progenitor cells give rise to morphologically and functionally diverse depots termed subcutaneous (SCAT) and visceral white adipose tissue (VAT) [1]. Depending on their localization within the body, both subtypes of white adipose tissue are termed differently and display distinct characteristics. SCAT is commonly divided into superficial and deep subcutaneous adipose tissue, and is more adept at energy storage, with greater plasticity in adipocyte

size, sensitivity to insulin signaling and responsiveness to antidiabetic thiazolidinediones (TZDs). In contrast, the visceral depots have mostly endocrine functions, respond with lipolysis to catecholamine signaling and uptake glucose upon stimulation by insulin. Owing to their endocrine activity and their implication in metabolic diseases, the visceral adipose depots have been extensively studied and targeted for therapeutic intervention.

White adipose tissue development has been attributed to mesenchymal cells and its expansion is parallel and twinned to angiogenesis. Its growth is based on enlargement of existing adipocytes but also in the differentiation of committed pre-adipocytes rising from endothelial cells of the inherent vasculature of the depot [5]. The master regulator of adipocyte differentiation, development and maintenance is the peroxisome proliferator-activated receptor γ (PPARγ) [1]. When activated, this nuclear hormone receptor drives both *in situ* maturation of preadipocytes as well as the migration of bone marrow-derived circulating progenitors to white adipose tissue sites and subsequent homing and expansion. Embryonic stem cells deficient in PPARγ and 3T3L1 cells of the pre-adipocyte line where the transcription factor is silenced with siRNA are unable to differentiate into adipogenic progenitors.

Total ablation of PPARγ is lethal in mice, as it leads to placental malformation. PPARγ heterozygous mice are normal overall save for a mild growth retardation in males induced by defective hormonal signaling. PPARγ+/- mice are protected from insulin resistance and liver steatosis in high fat diet experiments [6]. Studies of mice bearing the dominant-negative PPARγ mutation L466A in a heterozygous state exhibited increased sensitivity to high fat diet-induced steatosis, hyperinsulinemia and insulin resistance, which was reversed by thiazolidinedione (TZD) antidiabetic treatment [7]. Depletion of the transcription factor specifically in white adipose tissue protected mice from weight gain, maintained low serum levels of both leptin and adiponectin, and prevented the development of systemic insulin resistance in diet-induced obesity [8].

In humans, loss-of-function mutations in the PPARγ gene are linked with partial lipodystrophy. Familial partial lipodystrophy (FPL), one of the most commonly studied such conditions, selectively affects subcutaneous white adipose tissue depots of the extremities but not visceral and subcutaneous fat. The latter depots tend to increase in FPL patients, causing hyperinsulinemia, diabetes, increased triglyceride levels, hypertension, liver steatosis and polycystic ovarian syndrome [9].

In response to PPARγ activation, sprouting preadipocytes in mouse brown and white adipose depots gradually lose their endothelial characteristics and develop the signature of maturing adipocytes, with prominent expression of PPARγ, C/EBPα and C/EBPβ. PPARγ lineage-tracing experiments place the niche of adipocyte precursors within the vascular walls of adipose capillaries [5].

Apart from being responsible for adipose tissue development, PPARγ is also important for its function. It promotes free fatty acid release from circulating lipoproteins by regulating lipase expression, and stimulates free fatty acid uptake by enhancing the fatty acid translocase CD36 and the free fatty acid protein (FATP1) [10], [11]. Moreover, it is implicated in intracellular lipid trafficking by upregulating free acid binding proteins and facilitating the enzymatic esterification of fatty acids to form storable triglycerides [12]. Last but not least, it promotes the expression of fatty acid synthase, acetyl-coenzyme A synthase and stearoyl coenzyme A desaturase 1, thus regulating *de novo* free fatty acid synthesis [13].

The adipose tissue is a dynamic organ with the ability to expand and reduce its size and alter its morphology in response to nutrient influx, physiological changes in the organism, as well as environmental and neurological cues. It is innervated by efferent neurons of the sympathetic nervous system (SNS) sensitive to leptin signaling, which to some extent regulates lipolysis through sensory

circuits and feedback loops [14]. SNS-stimulated lipolysis and localized adipose injection of free fatty acids such as eicosanoidpentaenoic and arachidonic acid could increase adipose afferent nerve activity capable of triggering BAT thermogenesis, while the effect was abolished with surgical denervation of subcutaneous white adipose tissue.

2.2. The adipose tissue microenvironment in health and disease

The white adipose tissue can account for almost one quarter of the total body mass, being the organismal major source of nutrients. Adipocytes are the most prominent population in the tissue, and they have a unique morphology tightly directed from their lipid-storing function. Adipocyte nuclei are flattened and peripherally localized, while the majority of the cytoplasm contains lipids clustered in lipid droplet formations.

Lipid droplets consist of a hydrophobic core of neutral lipids enclosed by a phospholipid monolayer decorated with a specific set of proteins. They originate from the endoplasmic reticulum and can associate with most other cellular organelles through membrane contact sites. These contacts are highly dynamic and adapt to the cycles of lipid droplet expansion and shrinking. The biogenesis and degradation of lipid droplets, as well as their interactions with other organelles, are tightly entwined with cellular metabolism and are critical in regulating the levels of toxic lipid species [15].

Despite adipocytes, fat tissue contains an array of different cell types. Endothelial cells are abundant in the normal lean state, and are tightly associated with adipogenesis, as described earlier. The white adipose tissue is also rich in fibroblasts and surrounded by extracellular matrix components that maintain its morphology and accommodate its expansion upon lipid influx. The fat also contains a variety of immune cells, among which are T and B cells, macrophages, and dendritic cell subsets [16]. Interestingly, Tregs and resident macrophages co-localize in the lean adipose tissue, suggesting a potential role for Treg-mediated maintenance of immune homeostasis in the steady state [17], [18]. Disruption of the network of immune cells has been closely associated with obesity and can have either detrimental or beneficial effects on mammalian health.

In the lean adipose tissue, a collection of cytokines are naturally present, secreted either by adipocytes or resident immune cells [19]. The overall balance of pro- and anti-inflammatory signals tips the balance towards immune homeostasis in the lean state, with a prevalence of IL-4, IL-10 and IL-13, as well as high levels of adiponectin, an adipose-derived anti-inflammatory molecule with well described local and systemic effects.

During weight gain, adipocytes accumulate lipids. As the WAT expands, adipocytes increase leptin production to suppress food intake and limit the rate of triglyceride accumulation and adipocyte expansion. In obesity, the suppressive effect of increased leptin production is rendered moot by the development of resistance to leptin action. Leptin itself has pro-inflammatory effects, triggering the release of inflammatory cytokines by immune cells within the tissue, mainly TNFα. This pro-inflammatory landscape, along with the elevated insulin levels that accompany developing insulin resistance, feed the inflammatory loop promoting increased resistin production and further attenuate insulin sensitivity. Meanwhile, adiponectin production is prominently decreased in obesity, a change that might prime the tissue for establishment of the characteristic inflammatory state.

Instead of hyperplastic adaptation, adipocytes may instead become hypertrophic and die. Adipocyte death triggers innate immune responses characterized by the release of pro-inflammatory cytokines,

such as TNF, IFNγ, IL-1β and IL-6, into the tissue microenvironment [20]. This inflammatory remodeling is accompanied by extensive fibrosis and accentuated hypoxia which in turn lead to more extensive adipocyte death and vascular inflammation, feeding forward a circle of constant disruption of adipose homeostasis.

Adipocyte death has been attributed to pyroptosis and necrosis, though this still constitutes a matter for debate [21]. In both processes, however, rupturing of the plasma membrane leads to the release of intracellular contents into the adipose tissue microenvironment as danger-associated molecular patterns (DAMPs). Fatty acids, reactive oxygen species, nucleic acids, cholesterol and ATP attract phagocytic macrophages [22], which are in part recruited after myelopoiesis and monocytosis but also proliferate *in situ*. Macrophages surround dying adipocytes and form crown-like structures (CLS). They scavenge cellular debris and released lipids, often evolving into multinucleated or foam cells [23]. Pattern recognition receptors (PRRs) on macrophages, such as Toll-like receptors (TLRs) and NOD-like receptors (NLRs), instigate downstream signaling that results in inflammasome activation and proinflammatory cues via the MAPK and NF-kB pathways.

Although macrophages were the first immune cell type to be vilified for adipose tissue inflammation, a growing appreciation for other immune compartments gradually arises. Mast cells, neutrophils, eosinophils, natural killer cells and innate lymphoid type 2 cells (ILC2s) have been found to play significant roles in obesity-associated inflammation, in concert with cells of the adaptive immune system, namely NKT cells, B cells and T cells. This diverse artillery reflects the nature of the inflammation induced by obesity; a temporally complex, dynamic reaction.

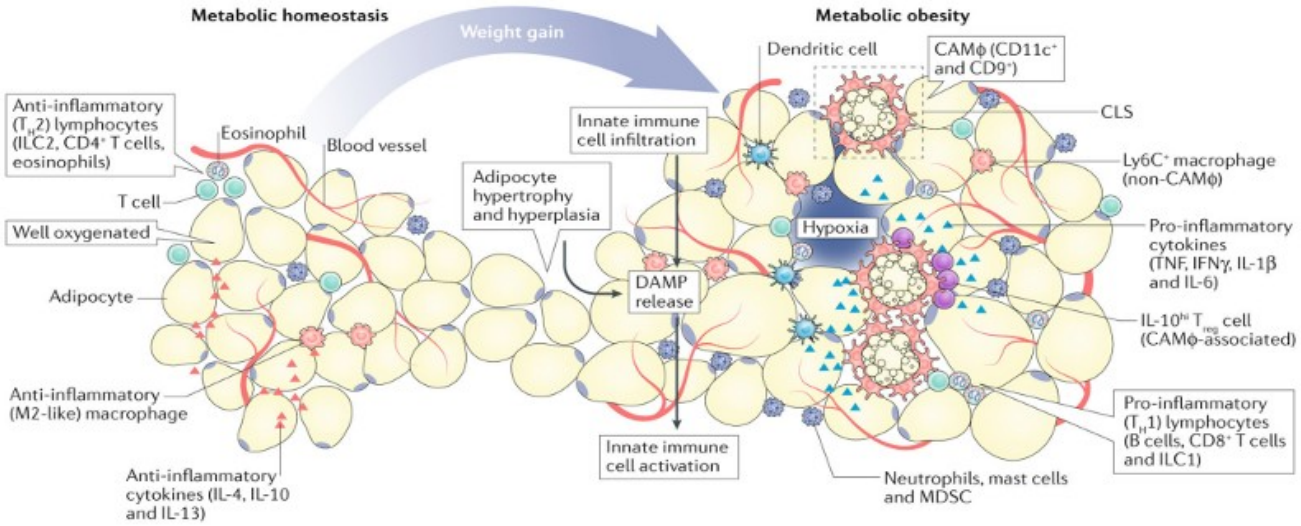

Figure 1. The white adipose tissue microenvironment in metabolic homeaostasis and metabolic obesity. In metabolic homeostasis, the adipose tissue comprises of adipocytes, endothelial cells, fibroblasts and adipocyte progenitors, as well as several resident immune cells of the innate and adaptive systems. The cytokine content and immune milieu overall maintain a dynamic equilibrium, and the tissue exhibits plasticity in response to metabolic, physiological and neurological cues. In metabolic obesity, adipocytes swell in response to lipid influx, become hypertrophic and die, releasing their contents as damage-associated molecular patterns (DAMPs) and triggering a local inflammation that gradually spreads to systemically impact the organism. Vascular inflammation and chronic fibrosis characterize the tissue, in a feed-forward loop that maintains a persistent, low-grade inflammation. *Image adapted from Quail & Dannenberg, Nature Reviews Endocrinology, 2018 [24].*

Adipose tissue macrophages promote myofibroblast activation and tissue fibrosis in obesity. This process is known as desmoplasia, and it involves extracellular components such as fibronectin and collagen deposition [24]. The vascular demand in growing adipose tissue mimics that of a growing tumour. Both tissues are highly vascularized, but vessel function is aberrant and insufficient to cover the metabolic demands [25]. Treg populations are diminished in obesity, alleviating homeostatic safeguards [17], [26], [27], and the loss of VAT Tregs might enable CLS expansion and shape a pro-tumorigenic landscape.

2.3 Regulatory T cells in different tissues

Peripheral Tregs are the dominant regulators of T cell immune responses against self and non-self antigens. As such, they prevent excessive inflammation during infection that would lead to autoimmune events and eliminate auto-reactive T cells that have not been eliminated during thymic development, ultimately maintaining immune homeostasis. Apart from T cells, Tregs are known to suppress the functions of innate immunity-related cells such as neutrophils, macrophages, dendritic cells, natural killer cells and innate lymphoid cells. Their significance as immunomodulators is exemplified in their absence; systemic Treg depletion typically induces immune-related autoimmune adverse events that manifest mainly as immunodysregulation polyendocrinopathy enteropathy X-linked syndrome (IPEX), characterized by Treg dysfunction, loss of suppressive activity, and subsequent autoimmunity.

Regulatory T cells exert their suppressive functions in an array of different mechanisms [28]. Cytokine-mediated suppression is a common characteristic of Tregs, and is achieved by secretion of anti-inflammatory molecules such as IL-10, IL-35 and TGFβ. Tregs can cause metabolic disruption in target cells via CD39:CD73 extracellular adenosine production and IL-2 deprivation, but can also directly induce cytolysis through granzyme B activity. Dendritic cell development is hindered via interaction with lymphocyte actiavtion gene 3 (LAG3), while the inflammatory functions of multiple target cells, such as other T cells and several types of antigen presenting cells, are inhibited via CTLA-4 and PD-1 inhibition [29].

The forkhead box P3 (Foxp3), also known as scurfin, belongs to the FOX protein family and is crucial in the development and function of regulatory T cells. As such, it is typically considered the master regulator of Tregs, and classical Treg populations are characterized by stable Foxp3 expression. Retroviral gene transfer of Foxp3 activates naïve T cells toward a regulatory T cell phenotype similar to that of natural regulatory T cells. That being said, the “one factor – one cell fate” theory has recently began to collapse, as evidence supports that Treg populations are in fact heterogeneous, and may also express transcription factors and other molecules that are typically associated with other T cell types. For instance, Tregs expressing the classical Th1 cell factor T-bet constitute a stable subpopulation of Tregs with increased suppressive activity in various infectious disease models.

Traditionally, Tregs are defined as CD4+Foxp3+ cells, with expression of Treg cell signature molecules such as CD25 and glucocorticoid-induced tumor necrosis factor receptor (TNFR)-related protein (GITR). Glucocorticoid-induced TNFR-related protein (GITR, CD357) in particular is indicative of Treg activation and has been targeted therapeutically for its Treg-depleting effects [30], [31]. Stable Tregs are characterized by a sustained Foxp3 expression, maintained suppressive function and hypomethylation of the CNS2 *cis* regulatory region within the *foxp3* locus. Disruption of Foxp3 expression leads to exhausted regulatory T cells with little to none suppressive action and upregulated

LAG-3 and TIM-3 exhaustion markers. These unstable Treg populations have been strongly associated with severe autoimmunity and tissue damage following cancer immunotherapy.

It is becoming abundantly clear that immune cells and molecules associated with immune responses serve an additional function; that of organismal homeostasis [32]. This new aspect of the immune system began with research on resident macrophages, but similar functions have been attributed to other immune cells. In particular, $CD4^+Foxp3^+$ regulatory T cells have been found resident in non-lymphoid tissues, among which the most extensively studied being Tregs in the skeletal muscle, the lamina propria of the intestine and the visceral adipose tissue.

Skeletal muscle regeneration is influenced by inflammatory events that accompany repair. An early, transient recruitment of neutrophils and myeloid-lineage mononuclear cells derived from a pool of circulating monocytes infiltrate acutely injured muscle, followed by M1-like macrophage responses that phagocytose debris. An M2-like macrophage population is then activated, responsible for remodeling of the damaged tissue and angiogenesis. Skeletal muscle-resident Tregs numbers rise in a fashion that temporally coincides with the switch in macrophage phenotype, originating both from within the inflammatory infiltrate of injured muscle as well as from between remote myofibers. Diphtheria-toxin-mediated ablation of Tregs in mice carrying a Foxp3-DTR allele compromises muscle regeneration, highlighting their importance in tissue repair.

Mice housed in non-germ free conditions host an abundant population of $Foxp3^+CD4^+$ T cells in their colonic lamina propria. The TCRs expressed by colonic Tregs are specifically reactive against fecal or cecal bacterial extracts, as well as against individual microbial isolates, and are considered as guardians of tissue homeostasis by suppressing resident or transiently present antigen-presenting cells and other T cells in the region. The two subsets found in the colonic region, classified as $ROR\gamma t^+Helios^{lo/-}$ and $Gata3^+Helios^+$ function as regulators of local immune responses and tissue remodeling, respectively.

Visceral adipose tissue-resident Tregs are the most studied population of non-lymphoid organ Tregs, serving as a paradigm of tissue-resident Tregs. They were first discovered in the epididymal VAT of lean mice, and have been attributed with maintenance of metabolic homeostasis. They comprise as much as 60-80% of the local $CD4^+$ compartment and have a transcriptome distinct from that of their lymphoid organ counterparts. Whole-genome expression profiling revealed thousands of transcripts significantly differentially regulated in VAT $Foxp3^+CD4^+$ T cells vis-à-vis those in the spleen or lymph nodes, which differ from each other by only a few hundred transcripts. VAT Tregs express diagnostic Treg markers like Foxp3, CD25 and GITR yet transcribe but about 65% of the canonical Treg signature. Among the classes of genes found up- and down-regulated in Tregs in the VAT most encode transcription factors, prominently PPARγ, chemokines and chemokine receptors, particularly CCR2, as well as cytokines and cytokine receptors like IL-10 and ST2. Most interestingly, a set of molecules implicated in lipid metabolism like low-density lipoprotein receptor (LDLR) and diglyceride acyltransferase (Dgat) are overexpressed specifically in VAT Tregs.

Tregs bearing this signature exhibit a unique phenotype and were highly enriched in the abdominal fat of normal mice, but their numbers were strikingly and specifically reduced at this site in insulin-resistant models of obesity [17]. Loss- and gain-of-function experiments revealed that VAT Treg cells influenced the inflammatory state of adipose tissue and therefore insulin resistance, while cytokines differentially synthesized by fat-resident regulatory and conventional T cells directly affected the synthesis of inflammatory mediators and glucose uptake by cultured adipocytes.

VAT Tregs display a distinct repertoire of antigen-specific receptors [33]. TCR clone 53 constituted 10% of VAT Tregs, and comprised of chains carrying the variable regions Vα2 and Vβ2, thus the team generated a TCR transgenic mouse line (vTreg53) on a *Rag*$^{-/-}$ background to avoid secondary rearrangements of the endogenous *Tcra* and *Tcrb* regions. Confirming their model in enrichment studies of VAT Tregs, they went on to label PPARγ and Foxp3 with fluorescent tags, producing a mouse line where VAT Treg origins could be traced. They demonstrated that Treg accummulation in the VAT was dependent on TCR specificity and Foxp3 expression, and also relied on cell-intrinsic IL-33 signaling. Their transgenic mice helped uncover a "two-step, two-site" pattern for acquiring the VAT Treg phenotype; CD4^{+}Foxp3^{+} thymic-derived Tregs undergo priming in the spleen, expressing low levels of PPARγ, before egressing the lymphoid organs into the periphery and becoming retained by means of TCR specificity into the visceral adipose tissue, from which point on their development and maintenance is mediated by local cues.

It was soon established that PPARγ, the master regulator of adipocyte differentiation and function, was responsible for the signature of VAT Tregs. Interestingly, both PPARγ isoforms co-immunoprecipitated with Foxp3 in transduced HEK293 cells, arguing that the transcription factors interact either directly or within a shared complex. Adenoviral induction of PPARγ and Foxp3 in naïve CD4^{+}CD25^{-} T cells in culture reprogrammed them towards a VAT Treg phenotype, while VAT Treg specific ablation of PPARγ abolished both the frequencies and the transcriptional fingerprint of epididymal VAT Tregs without affecting lymphoid or lung-resident Tregs [26]. It was also demonstrated that VAT but not spleen Treg cells readily took up lipids in high-fat treated mice, especially in response to treatment with pioglitazone, a PPARγ agonist and anti-diabetic medication of the TZD type. This process was characterized as PPARγ-dependent, as the drug induced the expression CD36 lipid transporter in wild type but not mutant mice. Taking into account that high fat diet in and of itself resulted in death and evacuation of typical VAT Tregs, the observation that abrogation of PPARγ expression in this context has no further effect was not surprising, and pioglitazone could not expand VAT Treg cells in mutant mice and was less effective than in the treatment of their wild-type counterparts at normalizing systemic metabolic parameters, as assessed by homeostatic model assessment of insulin resistance (HOMA-IR) and glucose tolerance tests.

Further experiments from the same research team evaluated the VAT Treg signature in different conditions and ages, and reported that it first appeared in the first 5 weeks of life in male mice, peaked with increasing age at approximately week 25 and gradually disappeared again as mice aged beyond the 40th week. The marked loss of VAT Treg numbers and their distinctive signature was similar to the phenomena observed in genetic and diet-induced obesity, bringing to context the term 'inflammaging' [34].

Most interestingly, the team discovered that it was the phosphorylation, and not the mere expression, of PPARγ on VAT Tregs that promoted their reprogramming. Diet-induced obesity is known to activate cyclin-dependent kinase 5 (Cdk5) and ERKs in adipocytes, leading to phosphorylation of the serine residue at position 273 (Ser273) of PPARγ. Certain PPARγ ligands, such as rosiglitazone, exert antidiabetic effects by blocking Cdk5-induced phosphorylation of PPARγ. These processes were detected in adipose tissue *ex vivo* and mimicked in TNFα-adipocyte cultures. The team hypothesized that the transcriptional profile induced by PPARγ Ser273 phosphorylation in adipocytes could function similarly in VAT Tregs, promoting the transcriptional patterns to which they owe their phenotype and function. Retroviral expression of *Foxp3* and *Pparg* was induced in conventional CD4^{+} T cells isolated from B6 mice and activated *in vitro* promoted the characteristic differential expression motif observed in VAT Tregs. Introduction of a mutant with an alanine substritution (*Pparg*-S273A) instead of the wild

type gene had no effect on conventional T cell reprogramming, and did not induce the VAT Treg signature. This effect was recapitulated in $CD4^+$ non-Treg cultures with addition of the Cdk5 inhibitor SR166.

The transcriptional profile of VAT Tregs discussed above comprises of several unique molecules. The transcription factors GATA3 and T-bet, traditionally considered as the master regulators of Th2 and Th1 immune responses, respectively, have been implicated in Treg stability and suppressive function, and were found increased in Tregs resident in the visceral adipose tissue [34]. More specifically, GATA3 is considered a marker for bona fide VAT Tregs, and is not expressed by lymphoid Tregs. Expression of both these transcription factors has been reported as a functional indicator of Treg suppressive potential, though T-bet is markedly downregulated in VAT Tregs compared to Tregs resident in other tissues [35]. Of note, both these markers are diminished in obesity.

The ectonucleotidase CD39 hydrolyses pro-inflammatory ATP, and on Tregs it is a marker indicative of highly active, highly suppressive, IL-10-producing cells in humans and mice [36]. Although levels of this molecule have not been evaluated in VAT Tregs, its expression by peripheral Tregs in relapsing-remitting multiple sclerosis is relevant to clinical outcome, and its role in IL-10-mediated Treg suppression highlights its importance. Human $CD39^{hi}$ Tregs exhibit increased stability and function, assessed by Foxp3 expression integrity under pro-inflammatory cytokine stimuli [37].In parallel, the ecto-5'-nucleotidase CD73 contributes to Treg inhibitory function via adenosine-mediated suppression of proinflammatory cytokine production by effector T cells [38]. T cell immunoglobulin mucin 3 (TIM3) is another co-inhibitory surface molecule associated with direct negative regulation of Tregs and a hallmark of T cell exhaustion [39]. Obesity induces its expression by Tregs, and the majority of intratumoral, but not peripheral, Tregs, highly express TIM3.

The IL33 alarmin receptor ST2 (suppression of tumorigenicity 2 receptor) is known to shape an immunosuppressive landscape in human tumors by facilitating Treg differentiation and promote a more migratory Treg phenotype [40]. It has been correlated with increased tumor size and adverse prognoses in human patients. In tumors, extracellular IL33 binds to ST2 enhancing the proliferation, evasion and migration of tumor cells, and exerts effects on endothelial cells thus promoting angiogenesis [41], [42]. Interleukin 33 (IL-33) signaling through ST2 and myeloid differentiation factor MyD88 was reported as an essential factor for the development and maintenance of VAT Tregs. It sustains their transcriptional signature via the transcriptional regulators BATF and IRF4, which are in turn necessary for direct regulation of ST2 and PPAR-γ expression. Notably, IL-33 administration induced vigorous expansion of VAT-Treg cells and improved metabolic parameters in obese male mice. In humans, omental adipose tissue Treg cells also highly express ST2, suggesting a requirement for IL-33 in VAT-Treg cell homeostasis that was evolutionarily conserved.

TNFR superfamily member OX-40 (CD134) is a co-stimulator found on T cells that augments immune responses against malignancies, and thus antagonistic antibodies targeting OX-40 are currently in clinical trials [28]. It promotes T cells survival, effector function mobility and memory, and is upregulated upon activation. It is also highly expressed on tumor-infiltrating Tregs in cancer such as melanoma, colorectal, head and neck cancer. Depletion of intratumoral Tregs using an agonistic antibody against OX-40 correlated with tumor regression in preclinical studies, though in clinical trials it led to a marked increase in infiltrating Treg frequencies.

Adherin-binding inhibitory receptor killer cell lectin-like receptor G1 (KLRG1) is expressed by a subpopulation of Treg cells with a $GATA3^+$ effector phenotype and functional plasticity conferring

protective effects in non-obese diabetic (NOD) mouse models [43] while impairing Treg fitness in tissues such as the intestine [44]. It has also been associated with NK cell cytotoxicity inhibition.

Recruitment of Foxp3+CD4+ T cells to parenchymal tissues reflects their response to chemokine gradients, and transcripts encoding many chemokine receptors are differentially expressed in tissue Tregs compared to their lymphoid-organ counterparts. Among those receptors, CCR2 is a chemokine reportedly overexpressed in VAT-resident Tregs and an important characteristic for their adipose tissue homing [45]. Interestingly, it has also been described as a potential chemoattractant driving Tregs to the microenvironment of some tumors.

2.4 The tumor microenvironment

Cancer and its associated comorbidities constitute one of the main causes of death worldwide, and cancer management has been a major concern for clinicians and researchers alike. Cancer immunotherapy is a promising strategy aiming to eliminate tumor cells by using the patient's own immune system. Vaccination, adoptive cell therapy (ACT) and immune checkpoint blockade are the three major approaches to date that are clinically employed for that purpose [46], [47].

Among these approaches, immune checkpoint blockade enhances the existing anti-tumor T cell immune responses. While the highly costly ACT harbors risks of TCRα- and β- chain mispairing, and while vaccination approaches remain highly non-specific, immune checkpoint blockade strategies pose none of those risks. Instead, they provide potential for long-term survival following treatment, and have been shown to be applicable to multiple cancer types [48], [49].

The tumor microenvironment has gained attention as a major factor contributing to cancer development and affecting response to therapy. The TME is unique, and comprises of many suppressive cell populations that hinder anti-tumor immune responses [46], [50]. With the disruption of tissue homeostasis in malignancy progression, the extracellular matrix and the stromal microenvironment are remodeled, in a process similar to that which occurs in obesity, desmoplasia. This effect is regulated by myofibroblasts and includes deposition of collagen and fibronectin [51]. Tumor microenvironments are loosely classified into three types based on the composition of the immune infiltrate and the character of the inflammatory response [52]. This classfication, though lacking in resolution, cellular heterogeneity and spatial distribution, can provide a diagnostic marker that informs the clinical decisions for immune checkpoint blockade (ICB) patient treatment.

Infiltrated-excluded (I-E) tumor microenvironments are associated with epithelial cancers such as colorectal carcinoma, melanoma and pancreatic ductal adenocarcinoma and are characterized by poor immunogenic potential as they are relatively void of cytotoxic T lymphocytes (CTLs). The observed CTLs lowly express activation markers, without fully infiltrating the tumor core, but instead accumulating in fibrotic nests in its borders. This prevention of immune responses is believed to be due to tumor-associated macrophages (TAMs) along the tumor margins. Infiltrated-inflammed (I-I) TMEs are characterized by high infiltration of PD-1- and PD-L1-expressing CTLs. Patients with I-I TMEs are more responsive to immune checkpoint blockade. A subclass of I-I microenvironments have been described to contain tertiary lymphoid structures (TLSs) and are therefore referred to as infiltrated-TLS TMEs. These lymphoid structures are generally located at the invasive tumor margin and the stroma, and are thought to act as sites of lymphoid recruitment and immune activation.

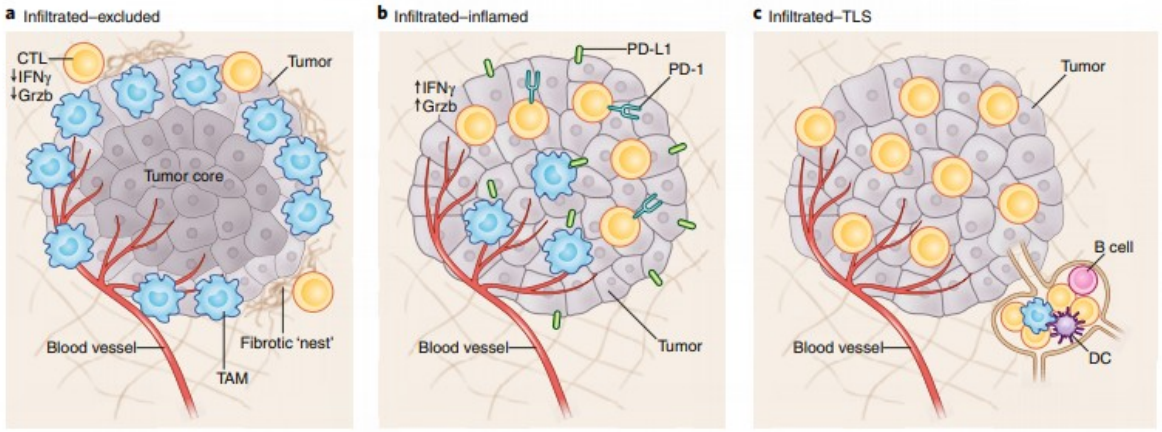

Figure 2. Types of tumor microenvironments. a, Infiltrated-excluded TMEs are considered immunologically 'cold', with limited CTL infiltration and poor clearance, **b,** infiltrated-inflamed microenvironments are immunologically 'hot', rich in pro-inflammatory molecules and highly expressing immune check molecules, **c,** infiltrated TMEs with tertiary lymphoid structures, a subcategory of infiltrated- inflamed microenvironments. *Image adapted from Binnewies et al, Nature Medicine 2018[52].*

One of the major hallmarks of cancer is the ability of tumor cells to evade immune responses. The unique tumor microenvironment is known to facilitate this escape from immune surveillance via several intricate mechanisms, the most prominent of which being the recruitment and activation of regulatory T cells within the tumor site. Thus, regulatory T cells which naturally suppress T cell responses and are responsible for maintaining immune homeostasis, inhibit T cell activation and tumor clearance [41]. Their numbers are elevated in the TME and peripheral blood of cancer patients across tumor types, shape a tolerogenic microenvironment and impair tumor antigen presentation [53]. They are abundantly recruited within tumor masses, utilize diverse suppressive mechanisms and target multiple cell subsets, thus posing a complex barrier to anti-tumor immunity and presenting a gross indicator of patient prognosis and responsiveness. The mechanisms behind their homing to tumors is still poorly

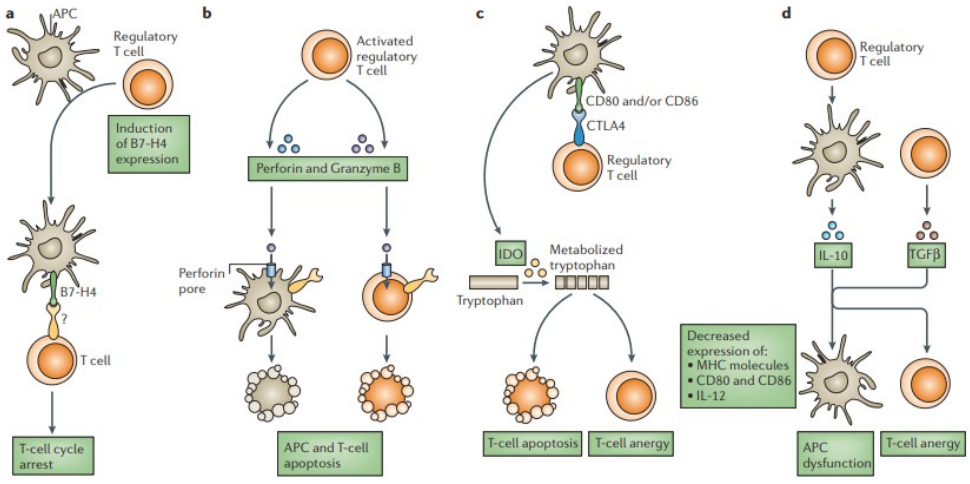

Figure 3. Treg suppressive mechanisms within the tumor microenvironment. a, Tregs induce B7-H4 expression by antigen-presenting cells, which in turn result in T cell arrest, **b,** Direct cell lysis induced by Tregs via perforin and granzyme B **c,** CTLA-4-mediated suppression and, **d,** cytokine-mediated Treg suppression. *Image adapted from Zou, Nature Reviews Immunology 2006 [29].*

understood, though evidence suggest host and Treg chemokines are implicated. Tregs adapt to the hypoxic microenvironment of solid tumors, are nurtured by tumor metabolites and display resistance to the reactive oxygen species (ROS) produced in these sites.

The paradigm shift in oncology that arose as our understanding of tumor immunity expanded with the emergence of immunotherapy found application in the therapeutic use of immune checkpoint inhibitors (ICIs) in the form of antagonistic antibodies against T cell inhibitory molecules, such as the cytotoxic T lymphocyte-associated protein 4 (CTLA-4) and the programmed death protein 1 (PD-1)/PD-L1 receptor-ligand axis [49]. Cancer immunotherapy aims at reinvigorating the patient's immune system and enhance its innate ability for tumor clearance instead of targeting cancer cells themselves, and has revolutionized both the clinical treatment of several cancer types and our basic knowledge of immunological responses to tumors. Depletion of regulatory T cells has found clinical applications, but progress is hindered by the fact that systemic disruption of Treg functions promotes severe autoimmune adverse events.

PD1 and CTLA4 are co-inhibitory ligands that downregulate the activation and impede the function of T cells. PD-1 is an inhibitor of TCR singaling expressed mainly by exhausted $CD4^+$ and $CD8^+$ T cells, but also by a fraction of Tregs, where direct interactions suppress $CD8^+$ cytotoxic cells expressing its ligand, PD-L1. It has been also associated with increased Treg stability and proliferation, particularly in human melanoma. Its blockade using monoclonal antibodies does not affect tumor Treg frequency [54]. CTLA-4 is constitutively expressed by Tregs and is integral to their function in part by mediating CD80/CD86 expression. Treg-specific CTLA-4 deletion has been associated with profoundly reduced suppressive capacity resulting in spontaneous systemic lymphoproliferation and fatal T cell-mediated immune disease [28].

Upon aPD-1 therapy IFNγ levels within the TME increase, mainly due to activation of CD8+ cytotoxic T cells. IFNγ is known to drive intratumoral Treg fragility, increasing IFNγ production without disrupting FoxP3 expression. Fragile Tregs are also sensitive to IFNγ, and overexpress its receptor, IFNγR1, though whether their fragile phenotype is a direct effect of aPD-1 or mediated by overall TME IFNγ levels is poorly understood, and several other mechanisms may exist that could promote Treg fragility. Treg fragility appears to be required for aPD-1 response in murine tumor models [55]. It is not yet clear whether that is also the case for human patients, and the idea that Treg fragility may be a key component in determining response to immunotherapy has been previously unappreciated.

Neuropilin-1 (Nrp1) has been found expressed by 90% of tumor infiltrating Tregs in mouse models of cancer and is critical for their function in the tumor microenvironment, although it seems dispensable in the maintenance of peripheral immune tolerance [56]. High levels of intratumoral NRP1+ Tregs correlate with poor prognosis in patients with melanoma and head and neck squamous cell carcinoma, while high Nrp1+ Treg populations in other cancer patients is associated with worse prognosis and disease-free survival. In murine models, Nrp1 depletion via genetic manipulation or antibody blockade promotes Treg fragility, yet whether this effect can also be observed in humans remains unknown. Interestingly, in the absence of Nrp1, fragility appears to be restricted within the TME. Nrp1 is known to associate with VEGF and promote angiogenesis, a fact that could explain the worse disease outcomes in patients and mouse models, as well as its brief consideration as a therapeutic target. However, the role of Nrp1 in the context of Treg fragility in humans has not been fully assessed.

2.5 The links between obesity and cancer

The link between chronic inflammatory conditions and cancer is widely appreciated. Obesity has been associated with both increased cancer incidence and progression across multiple tumor types, while it contributes to approximately 20% of cancer-related deaths [25]. Namely, epidemiological studies spanning the last four decades report increased incidence of endometrial and renal cell carcinoma in women, breast and colon cancer in postmenopausal women, while patients displayed decreased survival rates [57]. A landmark epidemiological study indicates that overweight and obesity are associated with mortality from a wide range of cancer types, and might explain 14% and 20% of all deaths from cancer in men and women from the United States, respectively. Additionally, a correlation of high body mass index (BMI) values and adverse cancer prognosis has also been reported in oesophagus adenocarcinoma, pancreatic cancer and tumors in the gastric cardia, the gallbladder and the liver of both men and women [58]. Partial lipectomy of parametrial fat in high-fat fed mice following a UVB-irradiation model for carcinogenesis inhibited keratoacanthoma and squamous cells carcinoma progression by stimulating cancer cell apoptosis [59]. Additionally, strong epidemiological associations link obesity with some lymphomas and leukemias. Overweight and obesity were associated with increased risk for malignant melanoma in males, as reported by a meta-analysis study [60], although the mechanisms underlying these observations remain unclear.

Several mechanisms have been proposed to explain the observed associations. For one, the proinflammatory landscape of the obese adipose tissue is believed to facilitate tumor growth and metastasis via cytokine secretion that promotes homing of metastatic cells to adipose tissue depots, and rapid growth of secondary tumors owing to the lipid-rich adipose setting [61].

Taking these observations into account, depots of white adipose tissue have been considered as potential targets for cancer prevention and treatment [3]. Both metabolic as well as inflammatory changes in the adipose tissue disrupt physiological homeostasis on a systemic level, and obesity-induced inflammation might underlie the described increased risks for cancer [25]. Although important correlations between metabolism and immunology in general have been revealed in recent years as an area worth exploring, little is actually known regarding the mechanisms underlying these observed connections. Paracrine communication between adipocytes and tumor cells has been discovered to occur in cancers that develop in close proximity to adipose depots, such as breast cancer [62]. In melanoma, SCAT adipocytes transfer lipids to tumor cells and promote melanocyte metabolic reprogramming and invasive capacity [63].

Often, the crude volume of adipose tissue is associated with increased disease risk, however it is the quality of adipose tissue expressed in inflammation status, adipocyte hypertrophy or hypoxia that constitutes the important factor commonly not accounted for. Metabolic dysregulation transcends simple weight measurements, as is exemplified by metabolically obese normal-weight individuals, who display metabolic abnormalities, such as insulin resistance, metabolic syndrome and increased all-cause mortality despite appearing lean. In addition, the marked differences between the biology and physiological roles of different fat depots should not be overlooked, as they differentially influence disease risk. For instance, evidence suggests that accummulation of white adipose tissue, particularly in the mesenteric and omental depots in humans, is strongly associated with metabolic abnormalities [64].

However, these associations have triggered skepticism within the scientific community, and evidence has arisen to suggest that overweight and early stages of obesity can also correlate with decreased tumor incidence and improved prognoses in some cases. The core of the criticism against the adverse

association of the two conditions lays namely in the fact that BMI is a crude tool for measuring obesity, vastly lacking in its sufficiency to establish metabolic dysfunction in all individuals, and further parameters should be tested to more adequately describe the obese phenotype, such as glucose tolerance and insulin resistance. Moreover, several confounding factors have been identified, such as carcinogen exposure, gender variations, reverse causality and collider bias [65].

A retrospective multi-cohort analysis of metastatic melanoma patients on different treatment regimes associated patient weights with survival outcomes [66]. Patients were stratified by BMI as underweight, normal, overweight and obese and observations spanned a decade (2006-2016). Different cohorts were analyzed for variance and meta-analyses were performed on the combined data for all patients. Among the therapies tested were targeted therapy (dabrafenib plus trametinib and vemurafenib plus cobimetinib), immunotherapy (ipilimumab plus dacarbazine and pembrolizumab, nivolumab, or atezolizumab) and chemotherapy (dacarbazine).

Obesity was associated with improved progression-free survival and overall survival compared to patients with normal BMI, and this association was dominant in male patients treated with targeted or immune therapy. Among patients prescribed ipilimumab, a blocker of CTLA-4 suppression, along with chemotherapy, obese ($BMI>30kg/m^2$) and overweight ($25<BMI<29.9kg/m^2$) displayed notably increased overall survival and distinct progression-free survival compared to normal individuals ($18.5<BMI<24.9kg/m^2$). This was also the case for patients receiving a-PD-1 immunotherapy as a monotherapy. These results were independent of traditional prognostic factors or concomitant medication, not confounded by differences in treatment tolerance, and appear to be sex-specific. These findings contradict associations between high BMI values and decreased survival rates previously published, however reverse causality due to treatment-related weight loss cannot be ruled out. Revealing as this evidence may be, no mechanistic explanations were provided in this study.

In response to this study, another research team attempted to investigate the paradoxical effects of obesity on T cell function during tumor progression and PD-1 checkpoint blockade [67]. Across multiple species and different tumor types, the reported survival advantage and improved responses to treatments of the a-PD-1/a-PD-L1 axis in obesity was recapitulated. In mice, it was established that obesity, both genetic and diet-induced, accelerated tumor progression with larger tumors that also were more metabolically active. The mechanism proposed for this was attributed to prominent T cell exhaustion development in obesity, expressed by high levels of PD-1. The main model used in this publication was B16.F0 melanoma, and the main focus was on $CD8^+$ T cells as they are known to provide a core anti-tumor defense mechanism. Exhaustion markers such as PD-1, LAG-3 and TIM-3 were markedly elevated in $CD8^+$ T cells of obese mice, while cytotoxic T cells also exhibited decreased proliferation rates within tumors. RNA sequencing analyses suggested that downregulation of activator molecules such as IFNγ, KLRG1 and granzyme B supplemented the exhausted identity of obese mouse tumors.

Since leptin exerts its effects via STAT3 signaling, and STAT3 binding sites are known to exist within the promoter region of the PD-1 gene, the team's experiments focused on leptin signaling and demonstrated that leptin is the main culprit inducing T cell aging. Moreover, the team suggested that it was this exhausted phenotype of $CD8^+$ T cells that rendered the obese tumors more susceptible to a-PD-1 therapy. Analysis of human data from the Cancer Genome Atlas (TCGA) revealed the exhaustion observed in mice was present in human colorectal cancers as well.

Although these studies propose invaluable insight regarding the correlations between obesity and cancer immunity, several questions remain unanswered as the underlying mechanisms remain vastly

unknown. Evaluating other cells implicated, discovering new molecules that have not yet been identified as markers for immune or metabolic status in both pathologies while acknowledging the inherent variations in the two conditions will help elucidate the network of interactions that drives the observed links, and propel both basic research of immunity as well as inform clinical practice.

3. Aim of Study

As discussed, Tregs have been studied separately in the context of both obesity and cancer, but no research results have been published yet linking the two conditions under the scope of Treg suppression. The aim of this study was to elucidate potential underlying connections between obesity and cancer in the context of regulatory T cell activity. This is of paramount importance if we consider that Tregs play an important role in tumor development and progression and also that VAT is a well established reservoir of Treg cells.

Our first objective was to evaluate the phenotype and molecular signature of fat-resident Tregs during tumor development. Previous tumor studies have focused on Tregs within the tumor microenvironment. There, Tregs exert suppressive effects, facilitating tumor immune evasion resulting to worse prognoses and decreased survival of patients. To date, no evidence exists regarding the effects of cancer to other tissue-resident, non-lymphoid Treg populations. Research on Tregs resident within visceral adipose depots of mice has identified the distinct fingerprint described in chapter 2, but has been limited to the context of obesity. In order to address this question, we designed a series of experiments to evaluate the profile of VAT Tregs following melanoma induction.

The second core objective of this study was to uncover how VAT Tregs may contribute to tumor development. Taking into consideration that VAT Tregs are strongly implicated and notably reprogrammed in obesity, we aimed at exploring the alterations in tumor progression and T cell responses this phenotype could instigate. We therefore designed experiments to assess the T cell landscape in the VAT, tumors and lymphoid organs of obese and lean mice, as well as the characteristics of Tregs in these tissues when tumors were induced in obese and lean mouse cohorts.

The role of intratumoral regulatory T cells in tumor immune evasion has been attributed to their ability to suppress T cell anti-tumor responses via immune checkpoint molecules, namely PD-1 and CTLA-4. Both are highly expressed in Tregs of the tumor microenvironment and are being clinically used as prognostic markers and as targets of immunotherapy regimes. Evidence linking obesity with higher cancer incidence is supplemented by the fact that metabolic dysfunction prompts $CD8^+$ T cell exhaustion indicated by increased PD-1 levels, conferring improved responsiveness to a-PD-1 and a-CTLA-4 approaches. Considering that the administration and effects of immunotherapy are systemic, it is likely that a VAT Tregs altered phenotype could influence its effectiveness. Thus, our final objective was to investigate the effects of VAT Tregs in immune checkpoint blockade.

In this study, we deemed it of value to examine these aspects of Treg function towards gaining further insight into the complex roles of Tregs in health and disease while remaining conscious of their clinical impact.

4. Materials & Methods

4.1 Mouse models

6-9 week old C57B6/J and Foxp3gfp.KI mice (on a C57BL/6 background) were kindly provided by A. Rudensky (Memorial Sloan–Kettering Cancer Center) [68] males and females were used for all experiments, unless otherwise specified.

4.2 Diet Induced Obesity

Obesity was induced by a lipid-rich diet (45kJ% fat (lard), Ssniff, E15744-344) provided in 10mm pellets for *ad libitum* feeding of 6-9 weeks. Free access to fresh water was allowed. Animals were age- and sex-matched and had statistically insignificant initial weight differences at experiment start. Control groups were kept on a normal 'chow' diet (10kJ% fat with no sucrose addition, Ssniff, E157452-04) for the same duration. Feeds were weekly replenished, while consumption statistics and weights were recorded every 6-10 days. After ~8 weeks of diet, when weights between cohorts differed significantly and glucose intolerance was established, cohorts were inoculated with B16F10 melanoma-inducing cells. Statistical analyses were performed with GraphPad Prism 6.

4.3 Glucose Tolerance Tests

Following overnight starvation of 16 hours, fasting glucose measurements were obtained by blood microsampling from the tail vein, using a blood glucose meter and strips (Contour, Ascensia SN1399895 0088 mg/dl 85892320 and 84745987). 1mg/g glucose (D-(+)-Glucose, anhydrous, 99%, Alfa Aesar A16828) was diluted in sterile PBS, filtered through 0.2μm filter and administered intraperitoneally to animals in 100ul/injections, and blood glucose values were acquired 15, 30, 60 and 90 minutes post glucose challenge. Values were analyzed using GraphPad Prism 6.

4.4 B16.F10 Cell Culture

Spontaneous C57BL/6-derived B16 melanoma is a well established and widely used tumor model for human melanoma, and several protocols for *in vivo* models of subcutaneous growth and pulmonary metastases have been described. When injected subcutaneously, B16 cells form palpable tumors between 5–10 days, and can grow to a $500mm^3$ tumor in 14–21 days. The most commonly used variant is B16.F10, a highly aggressive variant that will metastasize from a primary subcutaneous site to the lungs and colonize lungs upon intravenous injection to produce a high-fidelity lung metastasis model. In culture, B16.F10 form an adherent monolayer incorporating a mixture of spindle-shaped and epithelial-like cells [69].

B16F10 cells (ATCC ® CRL-6475™) were grown in RPMI (Gibco, 61870-010), complete with 10% FBS (Gibco, 10270106; heat-inactivated), 1% Penicillin/Streptomycin (Gibco, 15140-122) 0.01% β-mercaptoethanol (Gibco, 31350-010) in T75 flasks at 37°C, 5% CO_2. Cells were split at ~80-90% confluency, frozen in 10% DMSO (Dimethyl Sulfoxide for Cell Culture, AppliChem A3672.0050) in

FBS at a density of 2-3·10^6 cells/vial for storage at -80°C, and thawed into T75 flasks at the same density.

4.5 B16.F10 Melanoma Induction

At ~80% confluency, when B16F10 are typically in a phase of exponential increase, culture meda were discarded and culture monolayers washed with sterile PBS. Cells were harvested by addition of 2ml per T75 flask 0.25% Trypsin-EDTA solution (Gibco, 15400054) in PBS and incubation at 37°C for 3-5 minutes. Trypsin was inactivated by adding 10ml/flask complete RPMI and suspended cell clusters were reduced to single cell suspension by pipetting. Cell solutions were transferred to 50ml conical centrifuge tubes and precipitated (400g for 10 minutes at room temperature). Cell pellets were resuspended in 1ml sterile PBS and cells were counted in a Neubauer counting chamber, diluted 1:10 in Trypan blue solution (Gibco 15250061, 1:5 in PBS). Cell suspension volume was adjusted to a concentration of 300.000 live cells per 100ul injection.

Mice were anaesthetized with inhaled isofluorane (Isothesia, Henry Schein NDC 11695-6776-1) and shaved across the midback to facilitate inoculation and measurement of tumor growth at later stages. B16F10 cells were injected subcutaneously, very superficially, ensuring a visible, appropriate formation was shaped [69].

From days 9 through 15 p.i. (unless otherwise described), tumor volume values were obtained, using a caliper to measure perpendicular tumor diameters. Mice were sacrificed at the denoted days, when tumor volume ranged between 400-600mm^3. Tumor progression was visualized with curves using GraphPad Prism 6.

4.6 Tissue Collection

Animals were anesthetized with inhaled isofluorane, as described above, and blood from the retro-orbital vein was collected into 1.5ml microcentrifuge tubes.

For serum isolation, non-heparinized glass pasteur syringes were used, and blood was allowed to clot for ~30 minutes at room temperature prior to centrifugation (1500g for 10 minutes at 4°C). Topmost serum layer was collected and stored at -80°C.

For isolation of peripheral Tregs, blood was collected using heparinized glass pasteur pipettes and heparin-coated eppendorf tubes, and peripheral blood mononuclear cells were obtained using a ficoll gradient (Lymphocyte Separation Medium, LymphoSep, BioWest L0560-500) and centrifugation (400g for 20 minutes at room temperature, low acceleration and no breaks). Mice were euthanized immediately following blood collection by cervical dislocation.

Tumors were excised and cleared of skin and surrounding vasculature, weighed, and minced finely before enzymatic digestion (Collagenase D 100mg/ml, DNase V 10mg/ml) in 14ml round-bottom polypropylene tubes for 45-60 minutes at 37°C, pipetting every 10-15 minutes to facilitate tissue disruption. Subsequently, tumor homogenates were passed through 40μm cell strainers, washed with PBS and centrifuged (400g rpm, 10 minutes at 4°C). Tumor pellets were resuspended in appropriate volumes of 5% FBS in PBS for flow cytometry staining.

Tumor-draining inguinal lymph nodes were isolated, smashed and passed through 40μm cell strainer, washed with PBS and centrifuged (400g rpm, 10 minutes at 4°C). Cell pellets were resuspended in 2ml/sample 10mM ammonium chloride (NH_4Cl) hemolysis buffer to remove blood cells (NH_4Cl Scharlau AM 0270, KCO_3 PO 0173, EDTA (Titriplex III) PA AC 0965 in dH_2O, pH 7-7.4) for precisely 2 minutes, washed with PBS and centrifuged (400g rpm, 6 minutes at 4°C). Cell precipitates were resuspended in appropriate volumes of 5% FBS in PBS for flow cytometry staining.

Lymph node cellularity was measured. Cells were diluted 1:10 in Trypan Blue solution (1:5 in PBS) and counted in Neubauer counting chamber under an optical microscope. Cellularity per lymph node values were extrapolated for all samples.

Perigonadal fat pads were isolated, weighed and finely minced. As described above for tumors, enzymatic digestion (Collagenase D 100mg/ml, DNase V 10mg/ml) was performed in 14ml round-bottom polypropylene tubes for 45-60 minutes at 37°C, pipetting every 10-15 minutes to facilitate tissue disruption. Fat homogenates were passed through 40μm cell strainers, washed with PBS and centrifuged (800g for 15 minutes at 4°C) to separate and discard the upper adipocyte fraction. Supernatants were aspirated and the precipitated stromal vascular fraction (SVF) was resuspended in appropriate volumes of 5% FBS in PBS for flow cytometry staining.

4.7 Flow Cytometry

Staining panels using the antibodies below were designed for characterizing T cells from different tissues. Cytometric analyses and cell sorting were performed using a BD FACSAria™ or BD LSR II cytometer.

Samples were stained for extracellular markers by incubation at 2-8°C in the dark for 20-30 minutes with a final antibody concentration of 1ng/ml (unless otherwise stated). Tumor cell suspensions were vortexed briefly every 10-15 minutes to avoid clamping and ensure homogeneous antibody dispersion. Stained cells were washed with PBS and centrifuged (400g, 6 minutes at 4°C), and cell pellets were resuspended in 200ul 5% FBS in PBS for flow cytometry (stained intracellularly where needed).

Intracellular staining followed the extracellular staining protocol described above, and was performed using the Foxp3 Staining Buffer Set (eBioscience™, Cat. 00-5523-00). Fixation/permeabilization was achieved at 100ul/sample (4°C for 30-60 minutes), washes were made in 1X Wash Buffer in 1% BSA in PBS, and antibodies were diluted in 1X Wash Buffer to a final concentration of 4ng/ml for a 30-60 minute incubation at 4°C. After the final wash cell pellets were resuspended in 5% FBS in PBS.

Cytometric data were analyzed using FlowJo V10 for Windows OS.

Target molecule	Fluorochrome	Catalogue	Clone	Concentration
CD45.2	PerCP	Biolegend® 109826	104	1ng/ml
CD45	PE/Cy5.5	Biolegend® 103109	30-F11	1ng/ml
CD4	APC	Biolegend® 100412	GK1.5	1ng/ml
CD4	APC/Cy7	Biolegend® 100413	GK1.5	1ng/ml
CD25	APC/Cy7	Biolegend® 101918	3C7	1ng/ml
CD25	BV421	Biolegend® 102034	PC61	1ng/ml
Foxp3	Alexa488	Biolegend® 320012	150D	1:50 dilution
CD8a	PE	eBioscience™ 50-0081	53–6.7	1ng/ml
CD8a	PE/Cy7	Biolegend® 100722	53–6.7	1ng/ml
CD274 (PD1)	BV421	Biolegend® 135218	29F.1A12	1ng/ml
CD152 (CTLA4)	PE/Cy7	Biolegend® 106313	UC10-4B9	4ng/ml
CD152 (CTLA4)	PE	Biolegend® 106305	UC10-4B9	1ng/ml
T-bet	PE	Biolegend® 644810	4B10	1ng/ml
GATA3	BV421	Biolegend® 653814	16E10A23	1:200 dilution
CD304 (Neuropi1in-1)	PE/Cy7	Biolegend® 145212	3.00E+012	1ng/ml
CD39	PE	Biolegend® 143804	Duha59	1ng/ml
CD73	PE/Cy7	Biolegend® 127224	TY/11.8	1ng/ml
KLRG1 (MAFA)	APC	Biolegend® 138412	2F1/KLRG1	1ng/ml
ST2	BV421	Biolegend® 145309	DIH9	1ng/ml
CD134 (OX-40)	PE	Biolegend® 119409	0X-86	1ng/ml
CD223 (LAG3)	PE Dazzle	Biolegend® 125224	C9B7W	1ng/ml
CD357 (GITR)	APC	Biolegend® 126312	DTA-1	1ng/ml
CD192 (CCR2)	BV421	Biolegend® 150605	SA203G11	1ng/ml
CD366 (TIM3)	PE/Cy7	Biolegend® 134010	B8.2C12	1ng/ml

4.8 Cell Sorting for RNA Sequencing

Gonadal visceral adipose tissue SVF cell suspensions from Foxp3GFP mice were isolated and stained, as described above, for CD45 and CD4. $CD45^{+}CD4^{+}GFP^{+}$ Tregs were sorted and collected in tubes pre-coated with 20% FBS, washed with 5% FBS and precipitated (350g, 20 minutes at 4°C). Cell pellets were resuspended in RA1 buffer (RNA XS kit, NucleoSpim ® Macherey-Nagel 740902.50) and Tris(2-carboxyethyl)phosphine hydrochloride solution (TCEP, Sigma Cat. C4706) and stored at -20°C for RNA extraction.

4.9 Immunocytochemistry (ICC)

In order to define the best procedure for imaging both PPARγ and Foxp3 in VAT and, later on, tumors of obese mice to identify $PPAR\gamma^{+}Foxp3^{+}$ Tregs, imaging techniques were employed.

Our first approach was to stain cell extracts with the transcription factors of interest, before moving on to solving the issue of staining whole tissue. For these experiments, we included whole stromal vascular fraction (SVF) from total VAT of a B6 female (32 w.o.) as a positive control for PPARγ staining. $CD4^{+}CD25^{+}CD357^{+}$ Tregs sorted from the spleen of a B16-inoculated B6 female on day 14 of tumor progression was used as a positive control for Foxp3 staining. Splenic $CD4^{+}CD25^{-}CD357^{-}$ non-Tregs should be negative for both PPARγ and Foxp3, and were thus used as negative controls.

We followed the staining protocol suggested by aPPARγ (PPARγ Rabbit mAb Cell Signaling, C26H12, #2435) manufacturer. Briefly, cells were seeded to poly-L-lysine coated coverslips at a density of 100.000 cells per slip in 50ul PBS and incubated for 15 minutes at 37ºC. Fixation was achieved by addition of 500ul 4% PFA and incubation at room temperature for 15 minutes. Blocking was performed by immersion in PBS/1% BSA/0.3% Triton for 60 minutes at room temperature. Following three brief washes with PBS, primary antibodies were added (rabbit PPARγ mAb at a 1:500 dilution and mouse Foxp3, Clone 150D, 32001, BioLegend, at a final concentration of 1μg/ml). Primary antibodies were diluted in PBS/1% BSA/0.3% Triton and incubated overnight at 2-8ºC. Coverslips were washed with PBS and treated with secondary antibodies (goat a-rabbit AlexaFluor 647, far red, Invitrogen A21245 and goat a-mouse AlexaFluor 555, red, Invitrogen #A28180, both at final concentrations of 2μg/ml), diluted in PBS/1% BSA/0.3% Triton and incubated for 2 hours at room temperature. Coverslips were washed briefly with PBS and stained with DAPI (1:100) for 15 minutes at room temperature and mounted using 5ul poly(vinyl alcohol) mounting solution (Mowiol® Merck 81381). Cells were observed under a Confocal Leica TCS SP5 on a DMI6000 Inverted Microscope with dual tandem scanner and analyzed using ImageJ software for Windows OS.

It is important to note that no similar staining regimes for visceral adipose tissue have been published to date, and for this reason it was necessary to merge and fine-tune the protocols reported in other ICC protocols for the selected proteins in literature.

Since both PPARγ and Foxp3 are nuclear transcription factors, we sought to establish an optimal permeabilization approach prior to staining. Ultimately, we found that adding a permeabilization step (with 0.5% Triton in PBS for 15' at room temperature) provided more concrete results than Triton addition in all process buffers. To avoid the extensive background generated by Foxp3 staining we switched to a-mouse AlexaFluor 488 secondary antibody (Invitrogen A1159), while titration revealed that a final dilution of 1:1000 was optimal. In order to ensure staining specificity for PPARγ we calibrated imager settings using alternate control samples, and to intensify said specific signal we titrated primary aPPARγ antibody dilutions, concluding that a 1:20 dilution yielded the best results.

4.10 Imaging Tregs in epididymal Visceral Adipose Tissue

Several different approaches have been employed to stain immune cells in visceral adipose tissue depots, including OCT, paraffinization and perfusion [70].

VAT fat pads were isolated from DIO mice and fully immersed in fresh 4% PFA for 2 hours at 2-8ºC. Fat pads were thoroughly washed in PBS and incubated in 30% sucrose solution in dH_20, overnight at 2-8ºC. Tissue was carefully dried and immersed in optimal cutting temperature (OCT) mounting medium and frozen at -80ºC. 12μm sections were prepared in cryotome at approximately -27ºC and mounted on superfrost glass slides. Sections were incubated in glass bath of PBS for 10 minutes and washed briefly in PBS to remove OCT residues. Tissue sections were designated with a Pap Pen. We attempted two brief post-fixation steps using either 4% PFA for 5 minutes at room temperature or cold 100% acetone for 20 minutes at -20ºC. No difference was observed between the two post-fixation methods, and PFA additional fixation was decided upon for future protocols.

Blocking was achieved with incubation of sections in 3% BSA, 0.3% Triton, 0.3M Glycine for 60 minutes at room temperature (dark), to reduce background. Sections were then incubated overnight in primary antibody solutions (rabbit CD4 Invitrogen A5-87425 at a 1:100, rabbit PPARγ mAb C26H12, Cell Signaling at a 1:20 and mouse Foxp3 Clone 150D, 32001, BioLegend at a 1:10 dilution). Sections were subsequently briefly washed in PBS, and secondary antibodies were added (goat a-rabbit AlexaFluor 488 Invitrogen A11059 at a 1:500, goat a-rabbit AlexaFluor 647, far red, Invitrogen A21245 at a 1:1000 and goat a-mouse AlexaFluor 555, red, Invitrogen #A28180 at a 1:300 dilution) for 2 hours at room temperature (dark). After a series of brief washes with PBS, DAPI staining was performed (1:100 in PBS, 15 minutes at room temperature). Sections were washed and mounted with 5ul Diamond Mounting Medium (ProLong™ Gold Antifade Mountant, Invitrogen P10144).

Optimal dilutions of all antibodies described above were derived upon titration experiments.

Several studies on VAT report paraffin embedding as a more appropriate method for preserving and staining this distinct tissue [70]. Therefore, we obtained VAT fat pads from B6 females and incubated the samples in 10% formalin for fixation, overnight at 2-8ºC. Subsequently, samples were washed under running tap water and incubated in 30% sucrose solution overnight at 2-8ºC. Fixed preparations were preserved in 70% ethanol until paraffin embedding.

A histokinette tissue processor (Leica TP1020) was used for automated sequential incubations in increasing ethanol concentrations, xylene and paraffin preparations. Embedding in blocks was manually performed and blocks were stored at room temperature until sectioning. Sections were prepared on our behalf by the Histology department of Biomedical Research Foundation Academy of Athens (BRFAA), as was hematoxylin-eosin staining on VAT tissue sections.

Deparaffinization was achieved by serial incubations in xylene solution, following sequential incubations in decreasing concentrations of ethanol. Prior to staining, an antigen retrieval step was achieved by incubation of prepared sections in 10mM citrate buffer (Sodium citrate tribasic dihydrate Sigma 780100) at 80ºC for 10 minutes.

Both OCT and paraffin sections were observed with a Quantitative Photometry and Imaging system (PTI) and analyzed using ImageJ software for Windows OS.

5. Results

In our efforts to investigate the effect of a fat-enriched diet on tumor progression in relation to Treg cell function, we introduced a cohort of Foxp3gfp knock-in transgenic female mice to a high-fat diet, as described in chapter 4, while a second cohort of mice with similar weights was used as control. Body weights began to diverge from the first week of diet (Figure 4a), and on the sixth week of treatment when weights significantly differed, we inoculated both cohorts with B16.F10 melanoma-inducing cells and measured tumor progression over the course of fourteen days. Overall, the high fat diet cohort displayed the characteristics already reported in literature (Figure 4) [67]**.** Tumor progression was accelerated in the high-fat diet group as compared to the normal diet group (Figure 4b), though the differences were not statistically significant.

To better address the concept of obesity given that body weight is not sufficient to establish a metabolically dysfunctional state [25], we also performed a glucose tolerance test on a token number of mice from both cohorts one week prior to melanoma induction (Figure 4c). Though the sample number was too small to establish statistical significance, there is a distinct trend suggesting mild glucose intolerance in the high-fat-treated group (Figure 4c), a find that has been previously described [67].

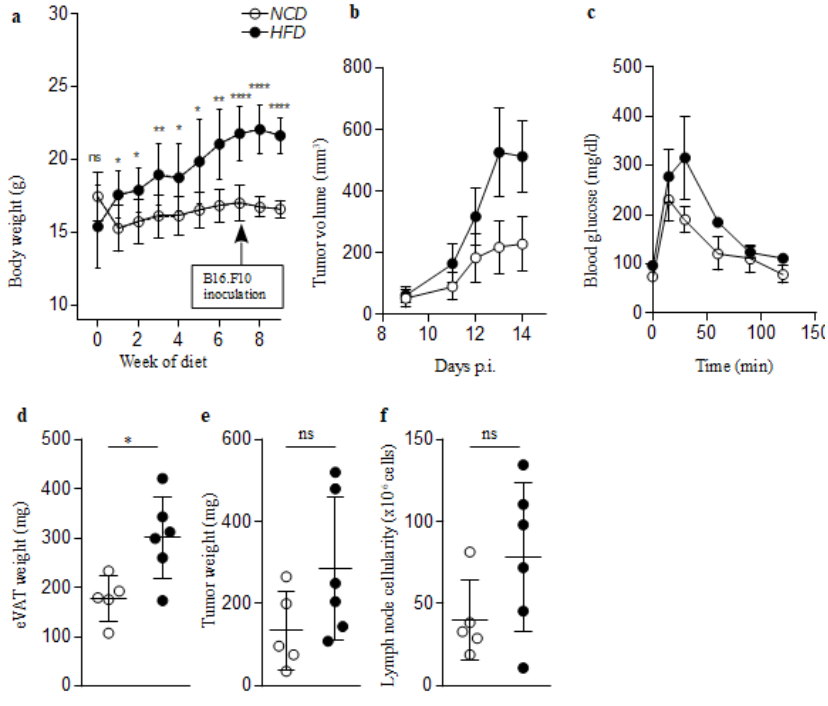

Figure 4. High fat diet accelerates tumor progression and increases cellularity of tumor-draining lymph nodes. a, weight gain per week of diet, **b,** tumor volume, **c,** glucose tolerance curve, **d,** epididymal fat pad weighs, **e,** tumor weights and **f,** lymph node cellularity per lymph node (inguinal). **p=0.0155, ns=not significant: unpaired, two-tailed, Student's t-test. Data are shown as mean ± s.d.*

Mice on a high-fat diet showed increased fat pad weights (Figure 4d) as a result of the lipid-rich diet. Tumor weights were notably increased in the high-fat group (Figure 4e), correlating with the observed accelerated tumor progression. As the tumor-draining lymph nodes are the major route of entry for tumor antigens, the increased lymph node cellularity observed (Figure 4f) suggests enhanced immune activity specific to the tumor challenge.

During melanoma progression, tumor antigens are drained into the inguinal lymph nodes and presented to lymphoid T cells, priming them for anti-tumor activity [71]. $CD8^+$ T cells are the major drivers of anti-tumor immunity, though $CD4^+$ effector T cells facilitate tumor control [49]. Flow cytometric analysis of cells isolated from the draining lymph nodes of the two cohorts revealed no significant changes in T cell subpopulations within

the tissue (Figure 5), indicating no qualitative differences in the immune responses to tumor challenge between the two groups as far as T cells are concerned. This observation did not change in our subsequent experiments.

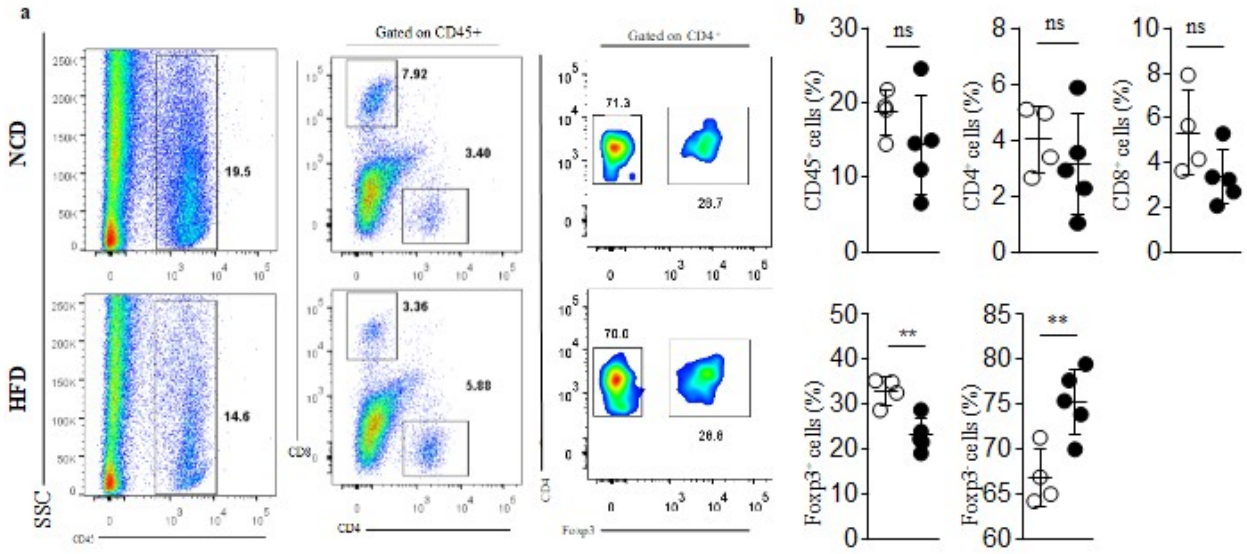

Figure 5. Obese tumors are characterized by altered lymphocyte infiltration. a, Gating strategy and **b,** population percentages of infiltrating lymphocytes. ***p=0.0036 (Tregs), **p=0.0083 (T effectors), ns=not significant: unpaired, two-tailed, Student's t-test. CD45$^+$: Mann-Whitney, two-tailed, U-test. Data are shown as mean ± s.d.*

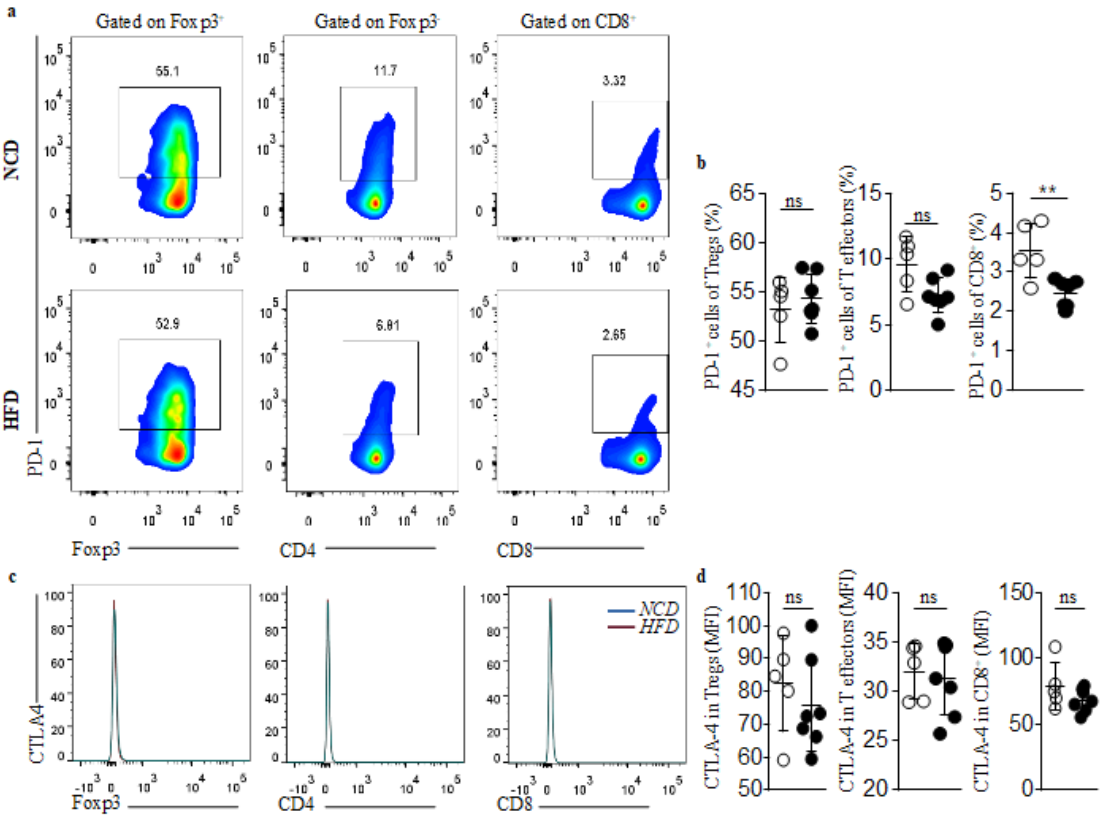

Figure 6. Obesity decreases PD-1 in T effectors and CD8$^+$ T cells of the lymph nodes, but has no effect on CTLA-4. a, Gating strategy and **b,** populations of PD-1$^+$ cells among tumor-draining lymph node T cell subpopulations, expressed as percentages of parent populations. **c,** Representative overlays and **d,** mean fluorescence intensity (MFI) of CTLA-4 in Tregs, T effectors and CD8 cytotoxic T cells. ***p=0.0054*, *ns=not significant: unpaired, two-tailed, Student's t-test. Data are shown as mean ± s.d.*

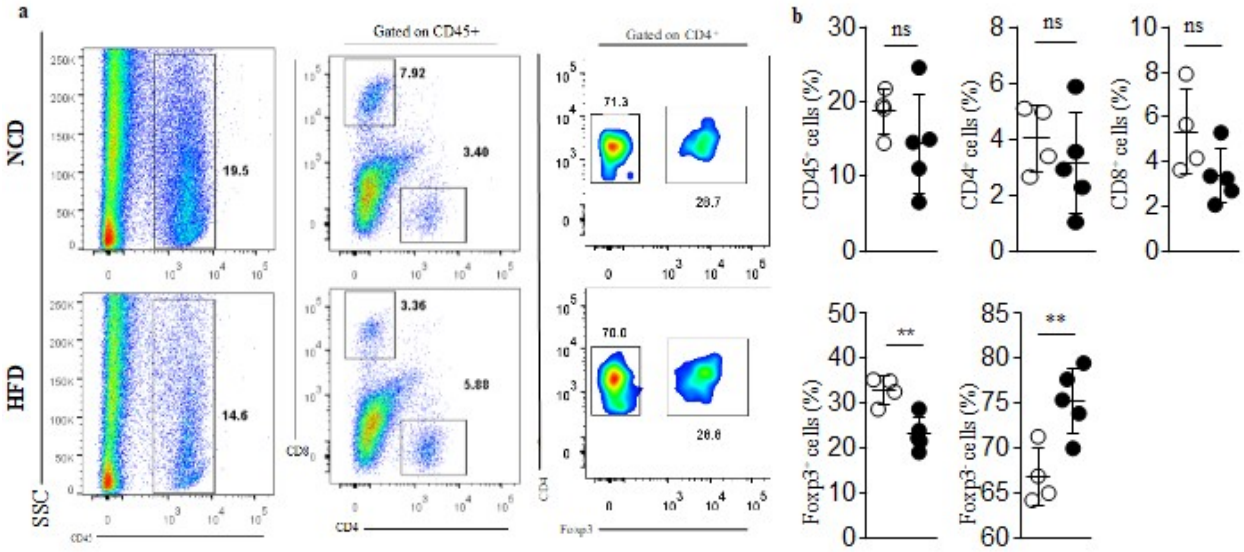

Figure 7. Obese tumors are characterized by altered lymphocyte infiltration. a, Gating strategy and **b,** population percentages of infiltrating lymphocytes. ***p=0.0036 (Tregs), **p=0.0083 (T effectors), ns=not significant: unpaired, two-tailed, Student's t-test. CD45$^+$: Mann-Whitney, two-tailed, U-test. Data are shown as mean ± s.d.*

Immune checkpoint blockade of PD-1 and CTLA-4 constitute FDA approved cancer therapies, and as discussed above obesity paradoxically correlated positively with responsiveness to checkpoint blockade regimes in melanoma patients [66], attributed to their overexpression in studies on mice [67]. Our analysis of PD-1 and CTLA-4 levels in different T cell populations in the lymph nodes (Figure 6) revealed a decrease in PD-1$^+$ on CD8$^+$ cytotoxic T cells that showed statistical significance in our subsequent experiments (Figure 6b). CTLA-4 is normally scarce and is known to be overexpressed in intratumoral Tregs [71]. Here, its levels were analyzed by means of fluorescence intensity (Figure 6c, d). No differences in CTLA-4 were observed for any of the T cell subsets studied, though a trend seemed to persist where CTLA-4 was generally lower in high-fat fed mice T cells upon tumor challenge. Conclusively, high-fat diet did not significantly alter T cell frequencies within tumor-draining lymph nodes in any of our experiments, and checkpoint molecules were comparable between the two groups except for a decrease in PD-1 on CD8$^+$ T cells, though this observation did not persist in our subsequent experiments.Tumors isolated from high-fat treated mice were characterized by decreased CD45$^+$ lymphocyte infiltration, a trend that was observed in our subsequent experiments on C57BL/6 female mice. Among the infiltrating lymphocytes, intratumoral Tregs were significantly decreased in obese females, while T effectors increased correspondingly (Figure 7).

As far as checkpoint molecules in the T cell subsets infiltrating obese tumors are concerned, PD-1$^+$ CD8 cytotoxic cells were generally lower (Figure 8a, b), while CTLA-4 levels did not display any significant differences (Figure 8c, d). Repeating these experiments will surely elucidate any underlying significance. All in all, the tumor T cell profile of high-fat diet mice suggest increased activity, though an overall decrease in the number of infiltrating total leukocytes correlated with the notable accelerated tumor progression.

The VAT-resident Treg signature has been extensively described in male mouse VAT [17], [26], [32], [34], [72]. As discussed in chapter 2, VAT Tregs overexpress the transcription factors PPARγ, GATA3 and T-bet, as well as the activation markers KLRG1, GITR and OX-40 and CD39. ST2 has been found to be integral to VAT Treg homing, maintenance and function, as is neuropilin-1. To date, no concise evidence has been published for female mice and intratumoral Treg phenotype. We studied the levels of these published molecules in tumor-infiltrating Tregs and visceral adipose tissue of high-fat and normal diet treated mice using flow cytometry (Figures 9-11). Additionally, we included the Treg suppression marker CD73 [38] and the co-inhibitor TIM-3 [39] to our analyses. However, since the number of Tregs

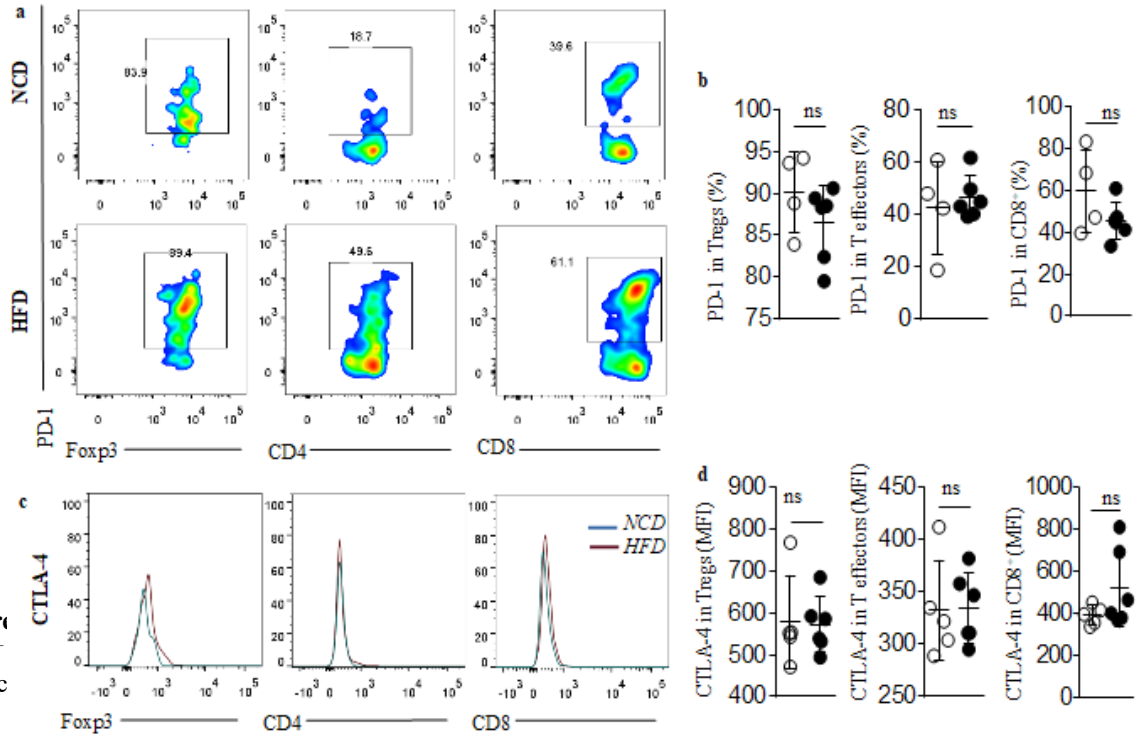

Figur ntages of
PD-1$^+$ ctors and
CD8 c

obtained from the VAT is generally very limited, we did not manage to obtain such information for VAT

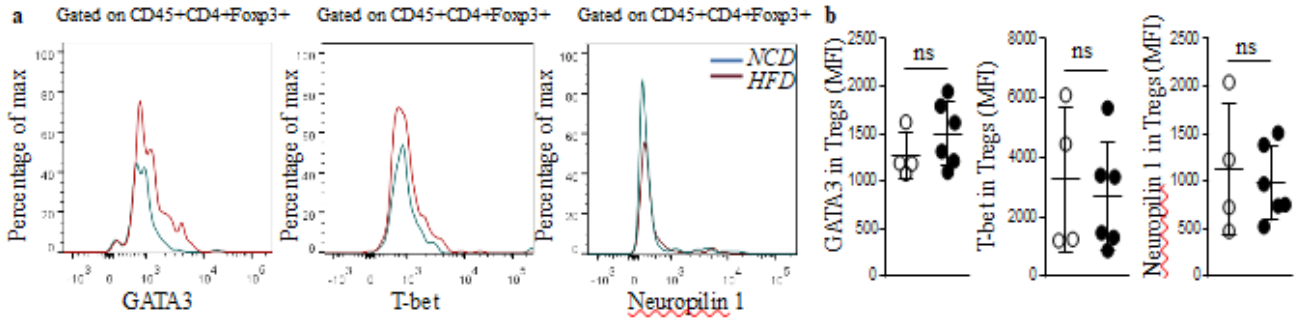

Figure 9. High-fat diet did not affect Treg stability upon melanoma induction. a, representative overlays and **b,** mean fluorescence intensity (MFI) in infiltrating T cell subsets. *ns=not significant: unpaired, two-tailed, Student's t-test. Data are shown as mean ± s.d.*

Tregs in our initial experiment, but only for tumors.

More specifically, we analyzed the levels of the transcription factors GATA3 and T-bet, as they have been implicated in Treg stability and suppressive function, and have been found increased in Tregs resident in the visceral adipose tissue [34]. In our Foxp3gfp female cohorts, no significant differences were found in these transcription factors between high-fat and normal diet treated groups (Figure 9a, b). The levels of neuropilin-1, also known to maintain Treg stability [56], did not differ between the two groups (Figure 9a, b). Still, repeating these experiments will reveal any underlying significance to these findings.

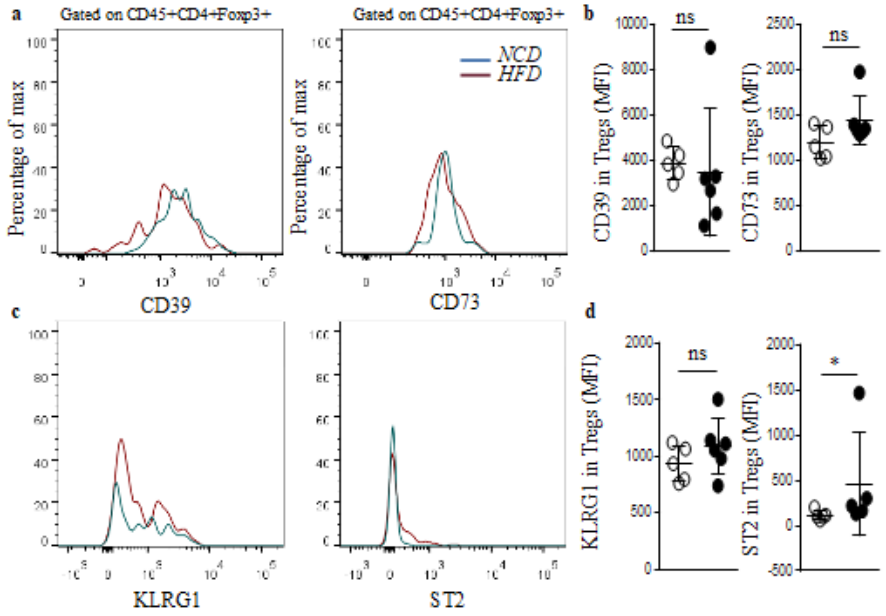

Figure 10. Decreased Treg activity in high-fat melanoma-bearing females. a, Representative overlays and **b,** mean fluorescence intensity (MFI) of CD39 and CD73 and **c,** representative overlays and **d,** mean fluorescence intensity (MFI) of KLRG1 and ST2 in tumor-infiltrating T cells subsets. **p=0.0317: Mann-Whitney, two-tailed, U-test; ns=not significant: unpaired, two-tailed, Student's t-test. Data are shown as mean ± s.d.*

The CD39 marker on Tregs is indicative of highly active, highly suppressive, IL-10 producing cells in humans and mice [36], [37]. In our experiment, CD39 showed a decreasing trend (Figure 10a, b), though repeating the experiment is necessary to establish it. The ecto-5'-nucleotidase CD73 contributes to Treg inhibitory function via adenosine-mediated suppression of proinflammatory cytokine production by effector T cells [38]. In the tumors of foxp3gfp females, no significant differences were observed in CD73 levels between the two groups (Figure 10a, b).

Adherin-binding inhibitory receptor killer cell lectin-like receptor G1 (KLRG1) is expressed by a subpopulation of Treg cells with a $GATA3^{+}$ effector phenotype and functional plasticity conferring protective effects in non-obese diabetic (NOD) mouse models [43] while impairing Treg fitness in tissues such as the intestine [44]. It has been associated with NK cell cytotoxicity inhibition [73]. In our study, we did not observe any differences in KLRG1 levels between the two groups (Figure 10c, d). The IL33 alarmin receptor ST2 (suppression of tumorigenicity 2 receptor) is known to shape an immunosuppressive landscape in human tumors by facilitating Treg differentiation and promote a more migratory Treg phenotype [40]. It has been correlated with increased tumor size and adverse prognoses in human patients. In tumors, extracellular IL33 binds to ST2 enhancing the proliferation, evasion and migration of tumor cells, and exerts effects on endothelial cells thus promoting angiogenesis [42], [68]. In the context of obesity, IL33 administration alleviated insulin resistance [72], and ST2 Tregs were increased in the VAT of lean male mice, and was required for Treg homing to visceral adipose depots. In the female mice studied here, ST2 showed an increasing trend in high-fat cohorts.

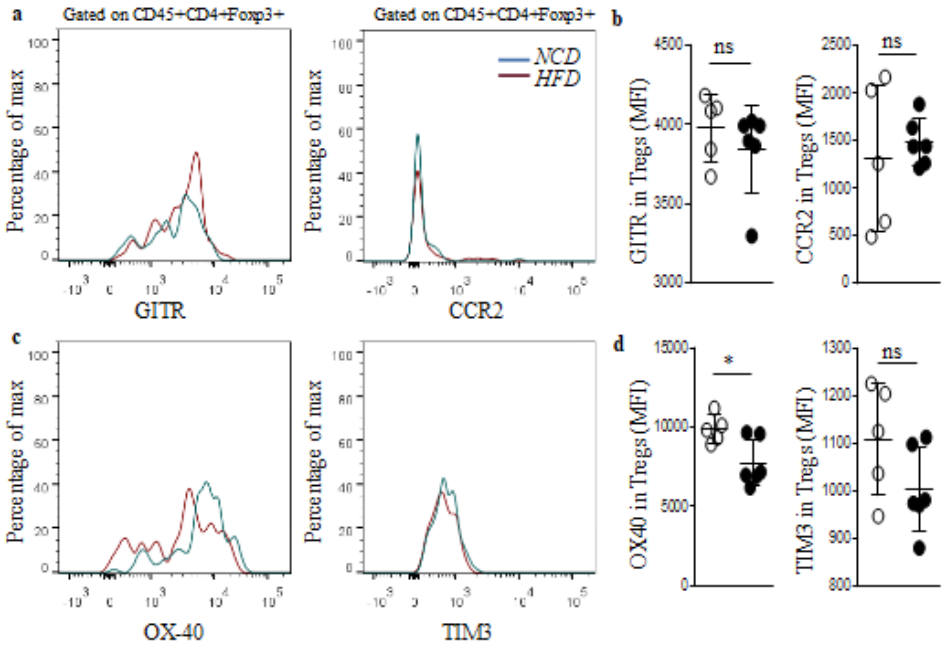

Figure 11. Decreased Treg activity in high-fat melanoma-bearing females. a, Representative overlays and **b,** mean fluorescence intensity (MFI) of GITR and CCR2 and **c,** representative overlays and **d,** mean fluorescence intensity (MFI) of OX40 and TIM3 in tumor-infiltrating T cells subsets. **p=0.0208, ns=not significant: unpaired, two-tailed, Student's t-test. Data are shown as mean ± s.d.*

Glucocorticoid-induced TNFR-related protein (GITR, CD357) of the TNFR family is another marker for Treg activation that has been targeted therapeutically for its Treg-depleting effects [30], [31]. In our experiments it showed a decreasing trend in high-fat cohorts (Figure 11a, b). CCR2 is reportedly overexpressed in VAT-resident Tregs and an important characteristic for their adipose tissue homing [45]. Here, there was a trend suggesting an increased $CCR2^{+}$ Treg population in tumors, though no statistical significance was established (Figure 11a, b).

Although our results so far suggest limited Treg function, OX40 (CD134), a co-stimulatory molecule abundant in the tumor microenvironment and known to augment immunological responses [28], was significantly decreased in the high-fat treated group (Figure 8c, d). Still, T cell immunoglobulin mucin 3 (TIM3), a co-inhibitory surface molecule associated with direct negative regulation of Tregs and a hallmark of T cell exhaustion [39] was reportedly notably lower levels on Tregs in the high-fat cohorts (Figure 11c, d). Although these results are representative of only one experiment, and further repetitions will be performed to elucidate the VAT Treg fingerprint, the trends observed suggest some similarities in the expression profiles of VAT Treg-specific molecules and tumors of obese female mice. The levels of markers for enhanced Treg suppression vary greatly, while molecules associated with Treg stability, such as neuropilin-1 and KLRG1 appear contradictive. Nevertheless, VAT Tregs from these mice were sorted for mRNA sequencing, and thus we expect more concise evidence that will inform future experiments.

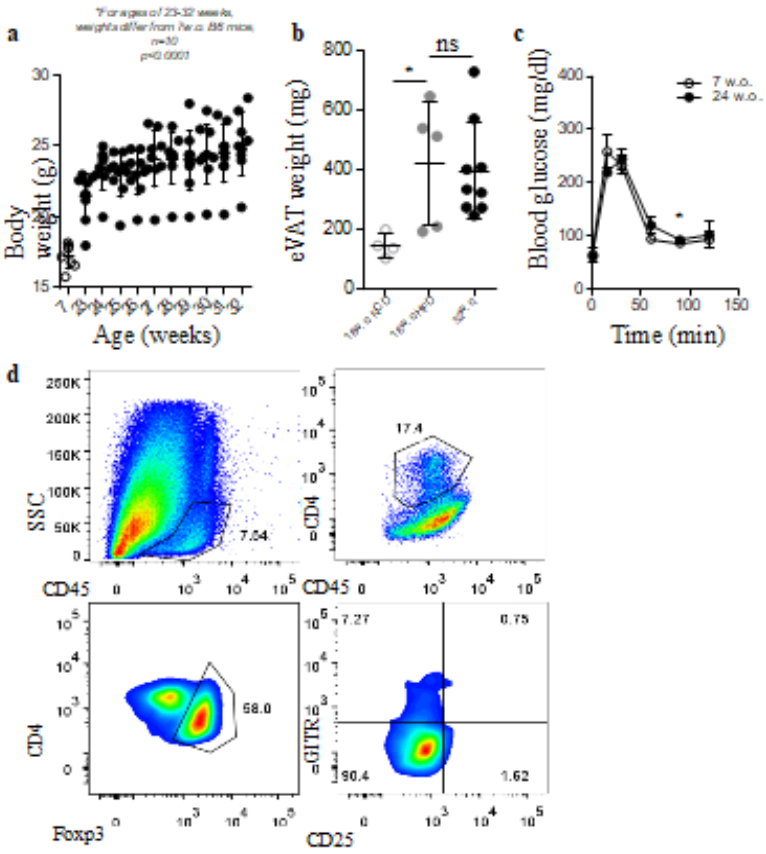

Figure 12. VAT Tregs in old female mice. a, Increasing body weights with age, **b,** Increased epididymal fat pad weights in aging and diet-induced obesity, **c,** Glucose tolerance test in 32w.o. and 7w.o. females, **d,** Gating strategy for identifying Tregs in the VAT. **p=0.0116, ns=not significant: unpaired, two-tailed, Student's t-test. Data are shown as mean ± s.d.*

The chronic, low-grade inflammation characteristic of obesity shows similar attributed to the inflammatory landscape in aging often referred to as "inflammaging" [74]. In lean male mice, VAT Treg cells increase between weeks 5 and 25 of age, then rapidly drop around the 40th week of life, while splenic Treg cells remain unaltered. This decrease with aging is accompanied by a decline in insulin sensitivity, suggesting a protective role of VAT Treg cells in aging-associated insulin resistance [34]. In order to discern whether this observation applies to females as well, but also to refine our protocol for VAT Treg isolation to ensure maximum yield, we measured the total

body weights (Figure 12a) and epididymal VAT weights (Figure 12b) of aging C57BL/6 females and observed expected statistically increases in both, while old female fat pad weights did not differ from those of corresponding 18 week-old cohorts on a high-fat diet. To better describe this phenotype, we performed a glucose tolerance test on 32 week-old and 7 week-old females (Figure 12c) and found that glucose tolerance in old animals was improved compared to obese cohorts already studied, though still exhibiting differences with the young animals. We also took this opportunity to standardize our protocol for isolating Tregs from eVAT, evaluating the levels of GITR and CD25, two markers characteristic of activated Tregs (Figure 12d).

With the protocol for Treg isolation from fat tissue established, we proceeded to repeat our initial experiment on C57BL/6 females. These cohorts displayed the same characteristics as Foxp3gfp females as far as body weights, VAT weights and tumor progression and weights had, albeit with a relatively slower overall tumor progression observed in both the treated and the control groups. Tumor-draining lymph nodes, tumors and eVAT were isolated and analyzed with flow cytometry.

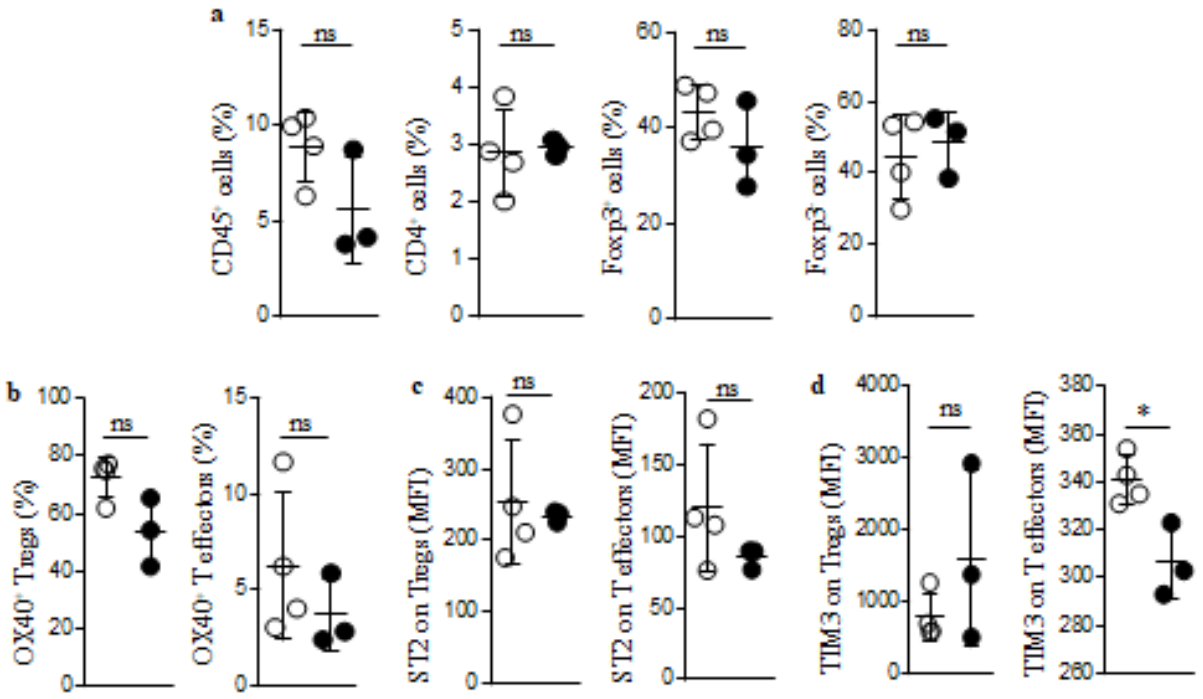

Figure 13. Immune landscape in C57BL/6 female VAT. a, $CD45^+$ and T cell populations within tumors of C57BL/6 females on a high-fat (black) and normal diet (white), **b,** $OX40^+$ Treg and effector T cell populations, **c,** Mean fluorescence intensity (MFI) of ST2 in Tregs and effector T cells, **d,** Mean fluorescence intensity (MFI) of TIM3 in Tregs and effector T cells. **p=0.0152, ns=not significant: unpaired, two-tailed, Student's t-test. Data are shown as mean ± s.d.*

In the fat samples, we found that CD45+ lymphocytes and Tregs slightly increased, CD8+ and effector T cells decreased (Figure 13a). The samples were pooled, a common practice in adipose tissue immune studies, making it impossible to evaluate our results statistically. Nonetheless, corresponding experiments from other members of the research team did manage to establish the decrease in VAT

Tregs as statistically significant. The trends observed in PD1 fluorescence persisted, while CTLA-4

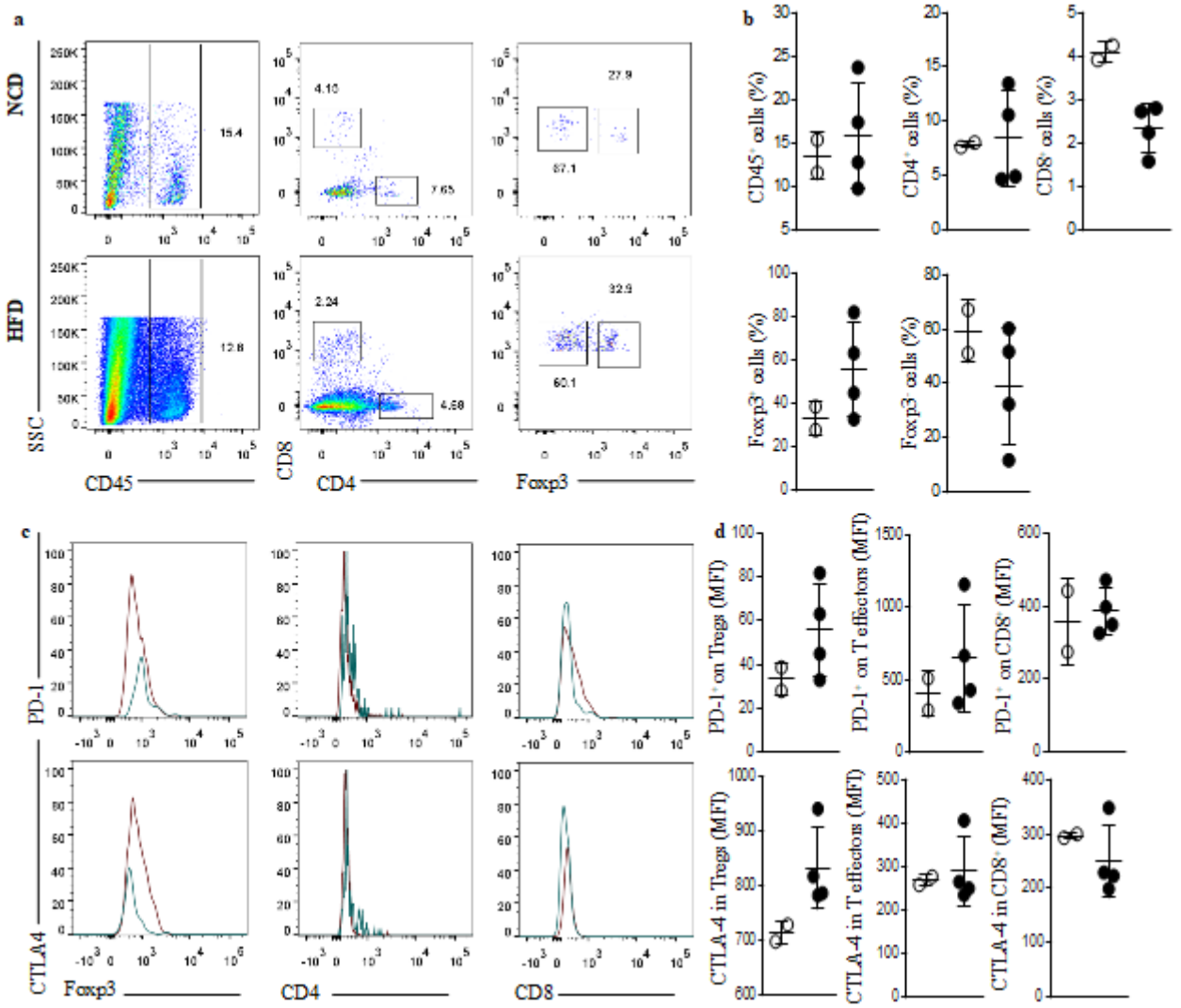

Figure 14. Immune phenotype of tumors in diet-induced obesity. a, Gating strategy and **b,** T cells populations in the epididymal fat. **c,** Representative overlays and **d,** mean fluorescence intensity (MFI) of PD-1 and CTLA-4 in eVAT T cells subsets. *Data are shown as mean ± s.d.*

showed no variation (Figure 13c, d).

In lymph nodes and tumors, results showed the same trends described above for the Foxp3gfp cohorts (Figure 14a). We focused our analysis on markers of the VAT Treg signature that had previously shown prominent variations between the two groups. OX40 was again decreased in Tregs of high-fat diet-fed females as well as in effector T cells (Figure 14b). Results on ST2 fluorescence were not recapitulated in C57BL/6 Tregs (Figure 14c), nor where those on TIM3 (Figure 14d), though the variance within each group was rather large in both cases. Notably, TIM3, whose expression on effector T cells infiltrating the tumor has been associated with short-lived effector populations, limited memory precursor differentiation and T cell exhaustion [75], was significantly decreased in high-fat females.

Comparing the total levels of PD-1 and CTLA-4 in Tregs and $CD4^+$ effector T cells in all our experiments, we do observe that PD-1 is more prominent in Tregs in the tumor-draining lymph nodes and tumors, as expected, though this effect is reversed in the VAT. CTLA-4 levels were higher in Tregs than T effectors in all tissues.

As discussed, the major regulator and most prominent characteristic of VAT Tregs is PPARγ. However, since no antibody for PPARγ exists for flow cytometric analyses, and sufficient protein extracts for western blotting from fat are hard to acquire, especially from females, we utilized imaging techniques in order to visualize it in adipose tissue immune cells and fat tissue. Imaging techniques in the adipose tissue pose challenges of their own, as the high lipid content makes frozen sectioning taxing and antigen retrieval necessary upon paraffin sample preparation can disrupt tissue integrity [70].

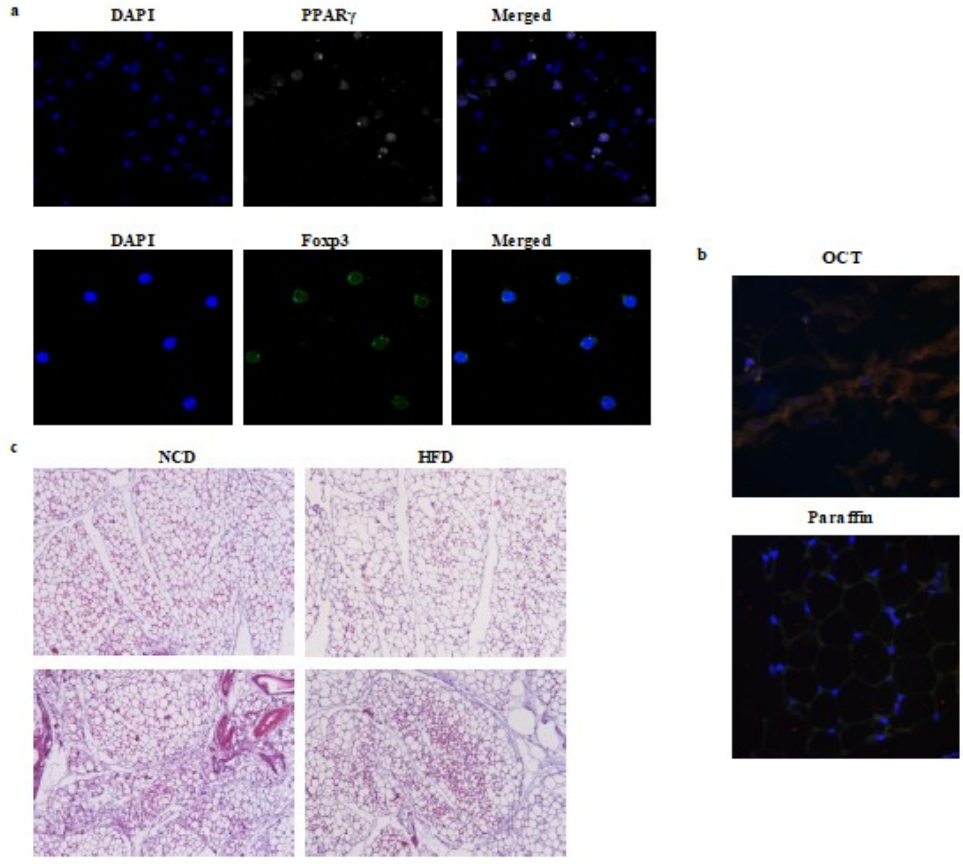

Figure 15. Imaging of eVAT stromal vascular fraction and tissue. a, Immunohistochemistry staining on stromal vascular fraction for PPARγ, 40X (top) and Foxp3, 63X (bottom) **b,** Tissue immunofluorescence on tissue sections, frozen sections (top) and paraffin sections (bottom), 40X, **c,** H&E staining on paraffin sections of eVAT (10X).

We employed different fixation protocols for stromal vascular fraction immunocytochemistry staining, and though the processes were improved and tailored to acquire adequate information, we did not obtain results on PPARγ and Foxp3 colocalization (Figure 15a). Though paraffin sections have been

considered with skepticism in studies of VAT, we found that tissue integrity was better preserved, even following antigen retrieval (Figure 15b). From the paraffin samples, we acquired hematoxylin-eosin stained sections to ensure tissue integrity and appreciate tissue structure (Figure 15c).

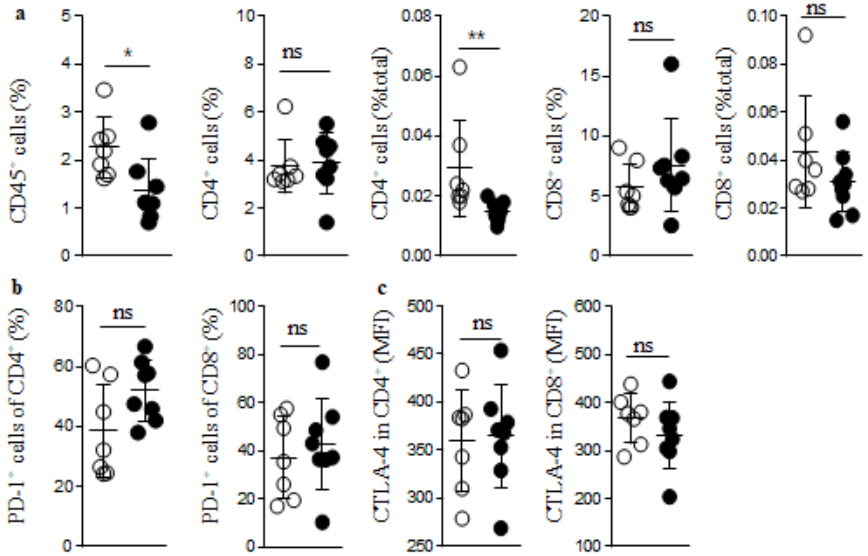

Figure 16. Reduced T cell activity in obese male tumors. a, $CD45^+$ and T cell populations within tumors of C57BL/6 males on a high-fat (black) and normal diet (white), **b,** $PD1^+$ cell frequencies among $CD4^+$ and $CD8^+$ T cells, **c,** Mean fluorescence intensity (MFI) of CTLA-4 in $CD4^+$ and $CD8^+$ T cells. **p=0.0185, **p=0.001, ns=not significant: unpaired, two-tailed, Student's t-test. ***p=0.0002: Mann-Whitney, two-tailed U-test. Data are shown as mean ± s.d.*

The fact that all studies on VAT Tregs in obesity are done in males and a recent publication that reported adipose tissue Treg imprinting is sex-specific and governed by gender hormones [76], prompted us to repeat our experiments on C57BL/6 males. As expected, initial weights in males were greater than in females, and weight gain was more prominent following diet-induced obesity (Figure 16a). Tumor progression showed a trend similar to females, though towards the final days of tumor challenge tumor volumes and weights upon sacrifice were comparable (Figure 16b). Epididymal fat pad weights were significantly larger in high-fat fed males, reflecting the rapid weight gain observed in total body weights and described in literature (Figure 16c).

Tumor infiltration by $CD45^+$ lymphocytes was prominently decreased, and among infiltrating T cells the percentages of total $CD4^+$ cells significantly lower (Figure 17a). No significant differences were observed in checkpoint molecules, though the same trends as in females appeared (Figure 17b, c). Due to technical difficulties, we did not observe Foxp3 fluorescence in this experiment. Overall, female weight gain, tumor progression and VAT characteristics exhibited the same trends that were observed in our experiments and have been described for males, though indeed the differences are less pronounced and would require further study for concrete observations to be reported.

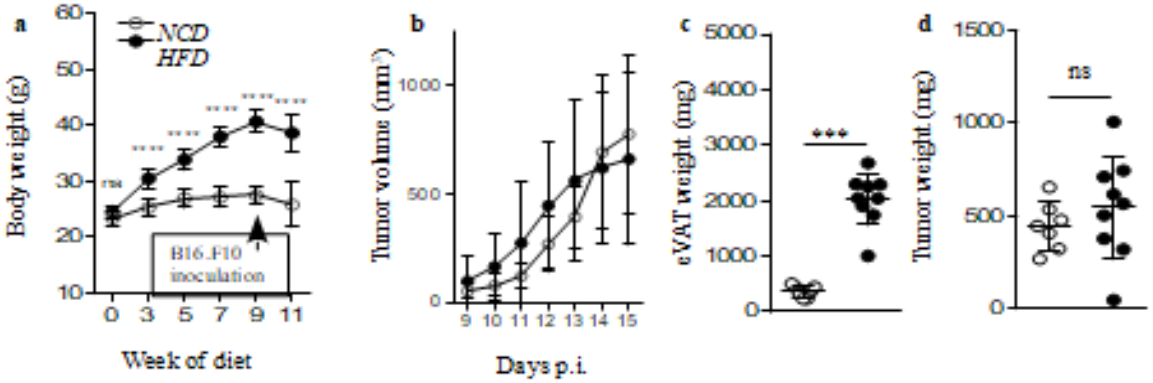

Figure 17. Male mice respond more promptly to diet-induced obesity. a, Total body weight gain, **b,** tumor progression, **c,** eVAT weights and **d,** tumor weights in C57BL/6 males on high-fat (black) and normal diet (white). *****p<0.0001, ns=not significant: unpaired, two-tailed, Student's t-test. ***p=0.0002: Mann-Whitney, two-tailed U-test. Data are shown as mean ± s.d.*

In the eVAT, $CD45^+$ lymphocyte frequencies were significantly increased in males, as were total $CD4^+$ (Figure 18a), indicative of the low-grade inflammation previously described for male mice, while checkpoint molecules did not show significant variation, though the trends observed in females persisted (Figure 18b, c).

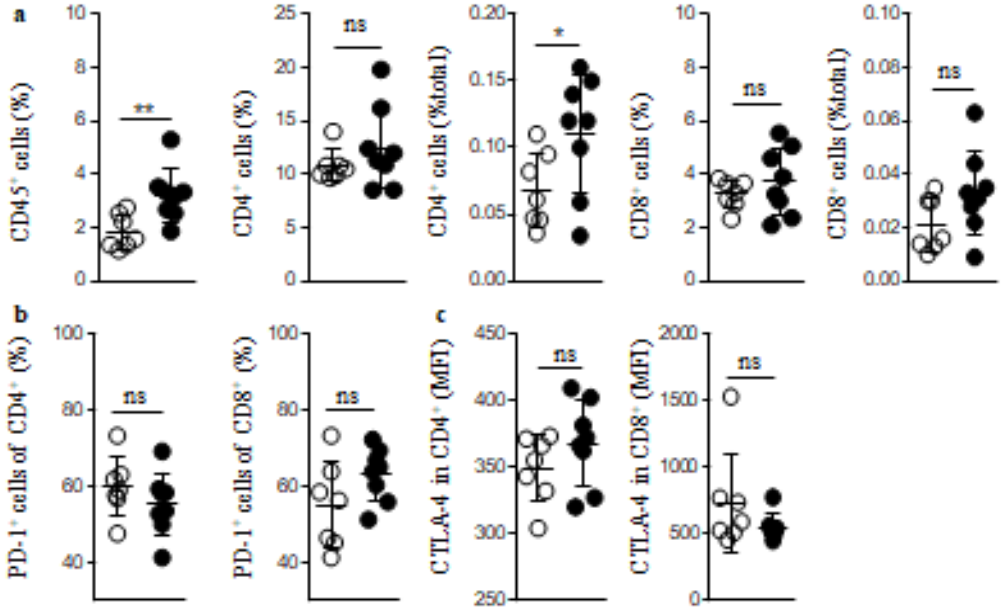

Figure 18. T cell populations and checkpoint molecules in obese tumor-bearing male VAT. a, $CD45^+$ and T cell populations within eVAT of C57BL/6 males on a high-fat (black) and normal diet (white), **b,** $PD1^+$ cell frequencies among $CD4^+$ and $CD8^+$ T cells, **c,** Mean fluorescence intensity (MFI) of CTLA-4 in $CD4^+$ and $CD8^+$ T cells. ***p=0.0085, *p=0.0490, ns=not significant: unpaired, two-tailed, Student's t-test. Data are shown as mean ± s.d.*

6. Discussion

Collectively, our results suggest that diet-induced obesity accelerates B16.F10 melanoma progression. These observations have already been published for male mice, as described in chapter 2, and our results replicated this phenotype in males but also revealed the same trends apply to females on a high-fat diet. Visceral adipose tissue depots increase in size, predominantly in males, consisting a larger proportion of the total body weight and tumor volumes are notably larger in high-fat treated mice of both genders.

Even though the total cellularity of the lymph nodes increases in tumor-bearing mice, especially so in the obese cohort, our results do not reveal any important alterations in the tissue immune composition. The frequencies of T cell subtypes, namely $CD4^+$ effector, $CD8^+$ cytotoxic and regulatory T cells in the tumor-draining inguinal lymph nodes did not show significant changes in any of our experiments, nor were checkpoint molecules affected by diet.

Our observations on tumors suggest a more immunogenic setting develops within obese melanomas. The ratio of Tregs over effector T cells was reduced in obese mice of both genders, even though total lymphocyte infiltration was diminished. PD-1 levels in $CD8^+$ T cells within the tumor microenvironment were noticeably lower, though CTLA-4 levels were not altered. This is at odds with the observed pronounced tumor progression, raising questions concerning the specific qualitative differences and the mechanisms underlying anti-tumor immunity in obesity. Such qualitative characteristics include but are not limited to altered immune cell metabolism, over- or under-expression of molecules that have yet to be identified as relevant markers, or cellular interactions that have not so far been demonstrated.

An increase in VAT Treg frequencies and decrease in effector and $CD8^+$ cytotoxic T cells suggest a more immunosuppressive landscape in the VAT of high-fat treated females. Total lymphocyte counts were slightly increased in obese female mice, though in males a reduction in VAT $CD45^+$ was observed, which has been previously described.

The VAT Treg signature examined in female tumors Tregs remains inconclusive, however, with different suppression markers over- and under-represented, and no capacity for definitive conclusions to be drawn regarding Treg stability and activation status. This gap in the knowledge is a major concern that will drive our future experiments.

Imaging of the adipose stromal vascular fraction and VAT tissue also proved challenging in this study. However, even though using immunofluorescent methods to visualize PPARγ Tregs in the VAT and in tumors would provide valuable insight into the interplay between obesity and melanoma from the scope of Tregs, it has been reported that it is PPARγ phosphorylation, and not expression, that is responsible for the VAT Treg phenotype. Thus, tools specific for pPPARγ identification should be employed to validate any observations from imaging results.

In designing this study, we chose to use a 45%kJ high-fat diet regime instead of the 60%kJ fat diet used in most studies. The reason behind this was the intention to recapitulate the natural progression of obesity in human populations as closely as possible. In this respect, though weight gain and the changes involved are decelerated in the lower fat content model, the validity of the results would be less likely to be compromised.

Moreover, we decided to focus mostly on the study of female mice, even though the associations examined have been better described in males where metabolic obesity is more prominent. This was

due to the fact that firstly, the tumor model has been extensively studied by the research team and expected tumor characteristics have already been established. Secondly, we were interested in exploring the potential divergence of phenotype between the sexes, and draw conclusions that would transcend gender variations.

Of note, the previous studies on tumor progression in the similar melanoma model discussed in the indtroduction utilized a less aggressive cell line to induce melanoma, resulting in delayed tumor progression, which still exhibited significant differences between normal and high-fat diet cohorts. However, the vastly larger cell numbers of B16.F0 injected in that study ultimately result in comparable tumor progression curves and similar melanoma volumes.

We fully understand that our series of experiments, having been standardized, should be repeated to uncover statistical importance that may be concealed due to increased variability within individual experiments. Currently, we have employed additional Foxp3gfp female cohorts while also focusing on evaluating steady state experiments that will describe the phenotype of VAT Tregs in B16.F10 melanoma regardless of diet, as well as describe the characteristics of Tregs in different adipose tissue depots in our model.

The decision to study VAT Tregss was based on the fact that they are the most characterized among tissue-resident Tregs, and are uniquely and profoundly affected by obesity when compared to Tregs in other fat depots. However, since VAT is distal to the subcutaneous melanoma model used, the question arose of whether subcutaneous adipose tissue (SCAT) depots which are also affected by a lipid-rich diet could affect tumor growth by proximity. Interestingly, preliminary experiments on subcutaneous adipose tissue in the model established and described above reveal a T cell milieu more similar to that of tumors than the VAT, and further experiments would aid in dissecting this observation and its potential implications.

Taking into account both the published literature and our initial results, we would hope to perform a more detailed characterization of the VAT Treg signature that was examined above, possibly including more molecules pivotal to Treg function. Namely, it would be interesting to assess the levels of inhibitory receptor LAG-3 (lymphocyte-activation gene 3, CD223), which is known to facilitate tumor immune evasion and is also a potential target for anti-tumor immunotherapy [77]. Another molecule of interest would be the scavenger receptor CD36, in light of recent evidence that intratumoral Tregs selectively upregulate it and develop metabolic adaptation to the lactic acid-rich tumor microenvironment via PPARγ-mediated mitochondrial fitness [78].

Interferon γ (IFNγ), a primary differentiation factor of $CD8^+$ T cells and a trademark molecule integral to the mediation of their cytotoxic effects [79], is also expressed in Tregs as a result of epigenetic reprogramming, and has correlated with instability of the suppressive population, making Treg IFNγ another target for further analysis [68]. Preliminary data from our research team reveal lower levels of the interferon in $CD8^+$ T cells infiltrating the tumors of obese mice, alluding to an attenuated anti-tumor immune response in concord with the already reported T cell exhaustion. It would therefore be essential to assess IFNγ levels in Tregs across tumors, lymphoid organs and adipose depots of obese melanoma-bearing mice.

Emerging evidence from our research team revealed limited $CD11b^+$ myeloid and $CD11b^+CD11c^+$ antigen presenting cell infiltration within obese tumors, which was accompanied by decreased MHC-II expression. Along with the increased frequencies of $CD11c^-CD11b^+Gr1^+$ myeloid-derived suppressor cells (MDSCs) observed in the obese TME, these results would render tumors less vulnerable to

immune checkpoint blockade, perhaps providing an additional tolerance layer. These observations and their possible implications are a reminder of the complexity of the tumor microenvironment, and propose additional targets for study alongside Tregs.

For example, dendritic cells have been implicated in cancer immunology, and even though they are rare within tumours and lymphoid organs, they have proven central for the initiation of antigen-specific immunity and tolerance [80]. A subset of dendritic cells, cDC1s are $CD11^{+}MHC\text{-}II^{+}$ and mediate cytotoxic immunnity. Together with our observations that MHC-II levels were lower in antigen presenting cells, analyzing their functionality in tandem with Tregs would provide further detail on the mechanisms implicated in our setting. Another interesting population is that of $CD4^{+}CD8^{+}$ macrophages. These cells are of a monocytic lineage and have been reported to exhibit cytotoxic activity, secreting Fas ligand, perforin and granzyme B and killing tumor cells in *in vitro* and *in vivo* rat syngenic NBT-II carcinoma model [81], [82].

MDSCs in the TME protect tumors from immune surveillance and are implicated in conferring resistance to immunotherapy, and have been found to promote the formation of Tregs [41], [83]. Furthermore, granulocytic MDSCs are elevated in the adipose tissue where they act protectively against insulin resistance. In breast cancer models, MDSCs upregulate PD-L1 during obesity, upon stimulation by tumor cell-derived IFNγ, facilitating tumor progression [84]. It would be informative to evaluate any possible implications of these cells in Treg suppressive function in our experimental setting.

It is understood that our research questions will not have definitive answers unless a tool to specifically deplete VAT Tregs is employed. Some published experiments utilize a fat-specific Treg depletion model, $Foxp3^{Cre}PPAR\gamma^{flox/flox}$ mice, where Tregs populations are diminished specifically in the VAT. This double transgenic mice were engineered based on the fact that PPARγ expression has been described as a defining event for VAT Treg homing, maintenance and function, and were critical in establishing this transcription factor as such.

All in all, the combined research of the interactions between metabolic and immune systems in concert with cellular metabolic aspects of immune cells is a blooming field referred to as organismal immunometabolism. This inclusive approach acknowledges the innate implications of different systems and their combined effects on health and disease. In this light, unveiling the underlying mechanisms defining obesity and its effects on tumor responses and immunotherapy effectiveness, as well as the possible implications of VAT Tregs in this interplay would serve a dual purpose. From a basic research perspective, it would be beneficial to understand in-depth the complex immune landscapes of both conditions and the interactions therein. From a clinical standpoint, the significance lies in refining immunotherapy regimes by identifying characteristics of metabolic states on an immunological level as a prognostic parameter to predict cancer outcomes and responsiveness to immunotherapy.

7. **Future Directions**

In spite of the acknowledged limitations, this project set the premises for further research regarding the role of VAT Tregs in tumor progression and immunotherapy. Still, several questions remain unanswered that would provide valuable insight into the subject.

As was discussed above, qualitative differences may underlie the observed phenomena even though quantitative variations in T cell subpopulations were not statistically significant. mRNA sequencing of Tregs sorted from fat depots, lymphoid organs and tumors of obese and lean Foxp3gfp mice should capture any changes that have not been revealed in the extent of published literature or the scope of this project. Gene enrichment analyses will help delineate the molecular mechanisms implicated in this setting, identify new potential markers for study and shed light on additional Treg cellular pathways involved, overall informing further experiments.

Despite the fact that VAT Tregs have been characterized in lean and obese conditions, functional assays have been challenging across scientific studies due to the few numbers acquired from the tissue and the limitations of Treg culture in general. Still, with large enough cohorts and using the benefits provided by the tool that are Foxp3gfp transgenic mice, we would hope to perform Treg suppression assays in our experimental setting, as well as evaluate the expression and protein levels of IL-10, a cytokine invaluable for Treg suppressive capacity [85].

To supplement the aforementioned considerations, immune checkpoint blockade experiments will be performed on high-fat treated versus control diet cohorts. Thus, we would be able to directly evaluate the effects of obesity on immunotherapy responsiveness, as well as the effects of immunotherapy on VAT Treg frequencies and phenotype variations.

Acknowledgments

As the author of this thesis I would like to kindly thank my supervisor, Professor P. Verginis, for his valuable guidance and immaculate mentoring throughout the duration of this project. I would also like to express my gratitude towards the members of the laboratory of Clinical, Experimental Surgery & Translational Research Center, BRFAA, as well as the Rheumatology laboratory in the School of Medicine, University of Crete, for their aid and supervision; the co-supervising faculty members, Professors C. Tsatsanis and C. Pontikoglou for their valuable insight and comments on the project; and lastly my family for their continuous support.

References

[1] S. I. Anghel and W. Wahli, “Fat poetry: A kingdom for PPARγ,” *Cell Research*. 2007.

[2] S. Michalakis and J. P. Zwolak, “Stability of Frustration-Free Hamiltonians,” *Commun. Math. Phys.*, 2013.

[3] E. D. Rosen and B. M. Spiegelman, “What we talk about when we talk about fat,” *Cell*. 2014.

[4] M. Khandekar, P. Nuutila, G. Schaart, K. Huang, H. Tu, and W. D. Van, “Beige Adipocytes are a Distinct Type of Thermogenic Fat Cell in Mouse and Human,” *Cell*, vol. 150, no. 2, pp. 366–376, 2013.

[5] K. Van Tran *et al.*, “The vascular endothelium of the adipose tissue gives rise to both white and brown fat cells,” *Cell Metab.*, 2012.

[6] J. Rieusset *et al.*, “Altered growth in male peroxisome proliferator-activated receptor γ (PPARγ) heterozygous mice: Involvement of PPARγ in a negative feedback regulation of growth hormone action,” *Mol. Endocrinol.*, 2004.

[7] W. He *et al.*, “Adipose-specific peroxisome proliferator-activated receptor γ knockout causes insulin resistance in fat and liver but not in muscle,” *Proc. Natl. Acad. Sci. U. S. A.*, 2003.

[8] J. R. Jones *et al.*, “Deletion of PPARγ in adipose tissues of mice protects against high fat diet-induced obesity and insulin resistance,” *Proc. Natl. Acad. Sci. U. S. A.*, 2005.

[9] A. K. Agarwal and A. Garg, “A novel heterozygous mutation in peroxisome proliferator-activated receptor-γ gene in a patient with familial partial lipodystrophy,” *J. Clin. Endocrinol. Metab.*, 2002.

[10] R. Avallone *et al.*, “A growth hormone-releasing peptide that binds scavenger receptor CD36 and ghrelin receptor up-regulates sterol transporters and cholesterol efflux in macrophages through a peroxisome proliferator-activated receptor γ-dependent pathway,” *Mol. Endocrinol.*, 2006.

[11] G. Martin *et al.*, “Induction of the fatty acid transport protein 1 and acyl-CoA synthase genes by dimer-selective rexinoids suggests that the peroxisome proliferator- activated receptor-retinoid X receptor heterodimer is their molecular target,” *J. Biol. Chem.*, 2000.

[12] I. Bogacka, H. Xie, G. A. Bray, and S. R. Smith, “The effect of pioglitazone on peroxisome proliferator-activated receptor-γ target genes related to lipid storage in vivo,” *Diabetes Care*, 2004.

[13] P. Tontonoz, E. Hu, J. Devine, E. G. Beale, and B. M. Spiegelman, “PPAR gamma 2 regulates adipose expression of the phosphoenolpyruvate carboxykinase gene.,” *Mol. Cell. Biol.*, 1995.

[14] J. T. Garretson, L. A. Szymanski, G. J. Schwartz, B. Xue, V. Ryu, and T. J. Bartness, “Lipolysis

sensation by white fat afferent nerves triggers brown fat thermogenesis," *Mol. Metab.*, 2016.

[15] J. A. Olzmann and P. Carvalho, "Dynamics and functions of lipid droplets," *Nature Reviews Molecular Cell Biology*. 2019.

[16] J. Lu, J. Zhao, H. Meng, and X. Zhang, "Adipose tissue-resident immune cells in obesity and type 2 diabetes," *Front. Immunol.*, vol. 10, no. MAY, pp. 1–12, 2019.

[17] M. Feuerer *et al.*, "Lean, but not obese, fat is enriched for a unique population of regulatory T cells that affect metabolic parameters," *Nat. Med.*, 2009.

[18] H. Zhou and F. Liu, "Regulation, Communication, and Functional Roles of Adipose Tissue-Resident CD4+ T Cells in the Control of Metabolic Homeostasis," *Frontiers in immunology*. 2018.

[19] J. R. Brestoff and D. Artis, "Immune regulation of metabolic homeostasis in health and disease," *Cell*. 2015.

[20] L. R. Howe, K. Subbaramaiah, C. A. Hudis, and A. J. Dannenberg, "Molecular pathways: Adipose inflammation as a mediator of obesity-associated cancer," *Clin. Cancer Res.*, 2013.

[21] A. Giordano *et al.*, "Obese adipocytes show ultrastructural features of stressed cells and die of pyroptosis," *J. Lipid Res.*, 2013.

[22] S. P. Weisberg, D. McCann, M. Desai, M. Rosenbaum, R. L. Leibel, and A. W. Ferrante, "Obesity is associated with macrophage accumulation in adipose tissue," *J. Clin. Invest.*, 2003.

[23] A. S. Haka *et al.*, "Exocytosis of macrophage lysosomes leads to digestion of apoptotic adipocytes and foam cell formation," *J. Lipid Res.*, 2016.

[24] M. Tanaka *et al.*, "Macrophage-inducible C-type lectin underlies obesity-induced adipose tissue fibrosis," *Nat. Commun.*, 2014.

[25] D. F. Quail and A. J. Dannenberg, "The obese adipose tissue microenvironment in cancer development and progression," *Nature Reviews Endocrinology*. 2019.

[26] D. Cipolletta *et al.*, "PPAR-γ is a major driver of the accumulation and phenotype of adipose tissue T reg cells," *Nature*, 2012.

[27] D. Kolodin *et al.*, "Antigen- and cytokine-driven accumulation of regulatory t cells in visceral adipose tissue of lean mice," *Cell Metab.*, 2015.

[28] T. Alissafi, A. Hatzioannou, A. I. Legaki, A. Varveri, and P. Verginis, "Balancing cancer immunotherapy and immune-related adverse events: The emerging role of regulatory T cells," *J. Autoimmun.*, vol. 104, no. July, p. 102310, 2019.

[29] W. Zou, "Regulatory T cells, tumour immunity and immunotherapy," *Nature Reviews Immunology*. 2006.

[30] D. A. Knee, B. Hewes, and J. L. Brogdon, “Rationale for anti-GITR cancer immunotherapy,” *European Journal of Cancer*. 2016.

[31] Y. Bulliard *et al.*, “Activating fc γ receptors contribute to the antitumor activities of immunoregulatory receptor-targeting antibodies,” *J. Exp. Med.*, 2013.

[32] M. Panduro, C. Benoist, and D. Mathis, “Tissue Tregs,” *Annu. Rev. Immunol.*, 2016.

[33] C. Li *et al.*, “TCR Transgenic Mice Reveal Stepwise, Multi-site Acquisition of the Distinctive Fat-Treg Phenotype,” *Cell*, 2018.

[34] D. Cipolletta, P. Cohen, B. M. Spiegelman, C. Benoist, and D. Mathis, “Appearance and disappearance of the mRNA signature characteristic of Treg cells in visceral adipose tissue: Age, diet, and PPARγ effects,” *Proc. Natl. Acad. Sci. U. S. A.*, 2015.

[35] F. Yu, S. Sharma, J. Edwards, L. Feigenbaum, and J. Zhu, “Dynamic expression of transcription factors T-bet and GATA-3 by regulatory T cells maintains immunotolerance,” *Nat. Immunol.*, 2015.

[36] N. Álvarez-Sánchez, I. Cruz-Chamorro, M. Díaz-Sánchez, P. J. Lardone, J. M. Guerrero, and A. Carrillo-Vico, “Peripheral CD39-expressing T regulatory cells are increased and associated with relapsing-remitting multiple sclerosis in relapsing patients,” *Sci. Rep.*, 2019.

[37] J. Gu *et al.*, “Human CD39hi regulatory T cells present stronger stability and function under inflammatory conditions,” *Cell. Mol. Immunol.*, 2017.

[38] M. S. Alam *et al.*, “ CD73 Is Expressed by Human Regulatory T Helper Cells and Suppresses Proinflammatory Cytokine Production and Helicobacter felis –Induced Gastritis in Mice ,” *J. Infect. Dis.*, 2009.

[39] K. Sakuishi *et al.*, “TIM3+FOXP3+ regulatory T cells are tissue-specific promoters of T-cell dysfunction in cancer,” *Oncoimmunology*, 2013.

[40] E. Pastille *et al.*, “The IL-33/ST2 pathway shapes the regulatory T cell phenotype to promote intestinal cancer,” *Mucosal Immunol.*, 2019.

[41] A. Hatziioannou, T. Alissafi, and P. Verginis, “Myeloid-derived suppressor cells and T regulatory cells in tumors: unraveling the dark side of the force,” *J. Leukoc. Biol.*, 2017.

[42] C. Schiering *et al.*, “The alarmin IL-33 promotes regulatory T-cell function in the intestine,” *Nature*, 2014.

[43] M. Kornete, E. Mason, R. Istomine, and C. A. Piccirillo, “KLRG1 expression identifies short-lived Foxp3+ Treg effector cells with functional plasticity in islets of NOD mice,” *Autoimmunity*, 2017.

[44] H. Meinicke, A. Bremser, M. Brack, K. Schrenk, H. Pircher, and A. Izcue, “KLRG1 impairs

regulatory T-cell competitive fitness in the gut," *Immunology*, 2017.

[45] J. E. Schoenhals, T. R. Cushman, A. P. Cadena, S. Demaria, and J. W. Welsh, "Immunomodulation with Radiation," in *Immunotherapy in Translational Cancer Research*, 2018.

[46] D. S. Chen and I. Mellman, "Review Oncology MeetsImmunology : TheCancer-ImmunityCycle," *Immunity*, 2013.

[47] Y. Choi, S. Lee, K. Kim, S. H. Kim, Y. J. Chung, and C. Lee, "Studying cancer immunotherapy using patient-derived xenografts (PDXs) in humanized mice," *Experimental and Molecular Medicine*. 2018.

[48] I. Mellman, G. Coukos, and G. Dranoff, "Cancer immunotherapy comes of age," *Nature*. 2011.

[49] D. M. Pardoll, "The blockade of immune checkpoints in cancer immunotherapy," *Nature Reviews Cancer*. 2012.

[50] D. Hanahan and R. A. Weinberg, "Hallmarks of cancer: The next generation," *Cell*, vol. 144, no. 5. Elsevier Inc., pp. 646–674, 2011.

[51] K. R. Levental *et al.*, "Matrix Crosslinking Forces Tumor Progression by Enhancing Integrin Signaling," *Cell*, 2009.

[52] M. Binnewies *et al.*, "Understanding the tumor immune microenvironment (TIME) for effective therapy," *Nat. Med.*, 2018.

[53] A. Tanaka and S. Sakaguchi, "Regulatory T cells in cancer immunotherapy," *Cell Research*. 2017.

[54] C. Stathopoulou *et al.*, "PD-1 Inhibitory Receptor Downregulates Asparaginyl Endopeptidase and Maintains Foxp3 Transcription Factor Stability in Induced Regulatory T Cells," *Immunity*, 2018.

[55] A. E. Overacre-Delgoffe and D. A. A. Vignali, "Treg Fragility: A Prerequisite for Effective Antitumor Immunity?," *Cancer Immunol. Res.*, 2018.

[56] G. M. Delgoffe *et al.*, "Stability and function of regulatory T cells is maintained by a neuropilin-1-semaphorin-4a axis," *Nature*, 2013.

[57] E. E. Calle, C. Rodriguez, K. Walker-Thurmond, and M. J. Thun, "Overweight, obesity, and mortality from cancer in a prospectively studied cohort of U.S. Adults," *N. Engl. J. Med.*, 2003.

[58] E. E. Calle and M. J. Thun, "Obesity and cancer," *Oncogene*. 2004.

[59] Y. P. Lu *et al.*, "Surgical removal of the parametrial fat pads stimulates apoptosis and inhibits UVB-induced carcinogenesis in mice fed a high-fat diet," *Proc. Natl. Acad. Sci. U. S. A.*, 2012.

[60] T. N. Sergentanis *et al.*, “Obesity and risk of malignant melanoma: A meta-analysis of cohort and case-control studies,” *Eur. J. Cancer*, 2013.

[61] K. M. Nieman *et al.*, “Adipocytes promote ovarian cancer metastasis and provide energy for rapid tumor growth,” *Nat. Med.*, 2011.

[62] Z. Zhang and P. E. Scherer, “Adipose tissue: The dysfunctional adipocyte- A cancer cell’s best friend,” *Nature Reviews Endocrinology*. 2018.

[63] M. Zhang *et al.*, “Adipocyte-derived lipids mediate melanoma progression via FATP proteins,” *Cancer Discov.*, 2018.

[64] T. McLaughlin, C. Lamendola, A. Liu, and F. Abbasi, “Preferential fat deposition in subcutaneous versus visceral depots is associated with insulin sensitivity,” *J. Clin. Endocrinol. Metab.*, 2011.

[65] H. Lennon, M. Sperrin, E. Badrick, and A. G. Renehan, “The Obesity Paradox in Cancer: a Review,” *Current Oncology Reports*. 2016.

[66] J. L. McQuade *et al.*, “Association of body-mass index and outcomes in patients with metastatic melanoma treated with targeted therapy, immunotherapy, or chemotherapy: a retrospective, multicohort analysis,” *Lancet Oncol.*, 2018.

[67] Z. Wang *et al.*, “Paradoxical effects of obesity on T cell function during tumor progression and PD-1 checkpoint blockade,” *Nat. Med.*, 2019.

[68] A. Hatzioannou *et al.*, “An intrinsic role of IL-33 in Treg cell–mediated tumor immunoevasion,” *Nat. Immunol.*, vol. 21, no. 1, pp. 75–85, 2020.

[69] W. W. Overwijk and N. P. Restifo, “B16 as a Mouse Model for Human Melanoma,” *Curr. Protoc. Immunol.*, 2000.

[70] G. Martinez-Santibañez, K. W. Cho, and C. N. Lumeng, “Imaging white adipose tissue with confocal microscopy,” in *Methods in Enzymology*, 2014.

[71] A. M. van der Leun, D. S. Thommen, and T. N. Schumacher, “CD8+ T cell states in human cancer: insights from single-cell analysis,” *Nature Reviews Cancer*. 2020.

[72] A. Vasanthakumar *et al.*, “The transcriptional regulators IRF4, BATF and IL-33 orchestrate development and maintenance of adipose tissue-resident regulatory T cells,” *Nat. Immunol.*, 2015.

[73] M. Ito, T. Maruyama, N. Saito, S. Koganei, K. Yamamoto, and N. Matsumoto, “Killer cell lectin-like receptor G1 binds three members of the classical cadherin family to inhibit NK cell cytotoxicity,” *J. Exp. Med.*, vol. 203, no. 2, pp. 289–295, 2006.

[74] C. FRANCESCHI *et al.*, “Inflamm-aging: An Evolutionary Perspective on Immunosenescence,”

Ann. N. Y. Acad. Sci., 2006.

[75] L. Avery, J. Filderman, A. L. Szymczak-Workman, and L. P. Kane, "Tim-3 co-stimulation promotes short-lived effector T cells, restricts memory precursors, and is dispensable for T cell exhaustion," *Proc. Natl. Acad. Sci. U. S. A.*, 2018.

[76] A. Vasanthakumar *et al.*, "Sex-specific adipose tissue imprinting of regulatory T cells," *Nature*, 2020.

[77] S. R. Woo *et al.*, "Immune inhibitory molecules LAG-3 and PD-1 synergistically regulate T-cell function to promote tumoral immune escape," *Cancer Res.*, 2012.

[78] H. Wang *et al.*, "CD36-mediated metabolic adaptation supports regulatory T cell survival and function in tumors," *Nat. Immunol.*, 2020.

[79] P. Bhat, G. Leggatt, N. Waterhouse, and I. H. Frazer, "Interferon-γ derived from cytotoxic lymphocytes directly enhances their motility and cytotoxicity," *Cell Death Dis.*, 2017.

[80] S. K. Wculek, F. J. Cueto, A. M. Mujal, I. Melero, M. F. Krummel, and D. Sancho, "Dendritic cells in cancer immunology and immunotherapy," *Nature Reviews Immunology*. 2020.

[81] T. Baba *et al.*, "CD4+/CD8+ macrophages infiltrating at inflammatory sites: A population of monocytes/macrophages with a cytotoxic phenotype," *Blood*, 2006.

[82] T. Baba *et al.*, " Rat CD4 + CD8 + Macrophages Kill Tumor Cells through an NKG2D- and Granzyme/Perforin-Dependent Mechanism ," *J. Immunol.*, 2008.

[83] R. J. Tesi, "MDSC; the Most Important Cell You Have Never Heard Of," *Trends in Pharmacological Sciences*. 2019.

[84] V. K. Clements, T. Long, R. Long, C. Figley, D. M. C. Smith, and S. Ostrand-Rosenberg, "Frontline Science: High fat diet and leptin promote tumor progression by inducing myeloid-derived suppressor cells," *J. Leukoc. Biol.*, 2018.

[85] X. Wei *et al.*, "Reciprocal Expression of IL-35 and IL-10 Defines Two Distinct Effector Treg Subsets that Are Required for Maintenance of Immune Tolerance," *Cell Rep.*, vol. 21, no. 7, pp. 1853–1869, Nov. 2017.